

We are IntechOpen, the world's leading publisher of Open Access books Built by scientists, for scientists

4,800

Open access books available

122,000

International authors and editors

135M

Downloads

Our authors are among the

154

Countries delivered to

TOP 1%

most cited scientists

12.2%

Contributors from top 500 universities



WEB OF SCIENCE™

Selection of our books indexed in the Book Citation Index
in Web of Science™ Core Collection (BKCI)

Interested in publishing with us?
Contact book.department@intechopen.com

Numbers displayed above are based on latest data collected.
For more information visit www.intechopen.com



Voltage-Gated Sodium Channels in Drug Discovery

Tianbo Li and Jun Chen

Additional information is available at the end of the chapter

<http://dx.doi.org/10.5772/intechopen.78256>

Abstract

Voltage-gated sodium channels (Nav) control the initiation and propagation of action potential, and thus mediate a broad spectrum of physiological processes, including central and peripheral nervous systems' function, skeletal muscle contraction, and heart rhythm. Recent advances in elucidating the molecular basis of channelopathies implicating Nav channels are the most appealing druggable targets for pain and many other pathology conditions. This chapter overviews Nav super family from genetic evolution, distribution, human diseases/pathology association, highlighting the most recent structure function breakthrough. The second section will discuss current small and large Nav modulators, including traditional nonselective pore blockers, intracellular modulators, and extracellular modulators.

Keywords: voltage-gated sodium channel, Nav1.7, drug discovery

1. Introduction

Voltage-gated sodium channels (Nav) are large transmembrane proteins that conduct the flow of sodium ions down the electrochemical gradient through cell membranes. In excitable and nonexcitable cells, these channels control action potential initiation/propagation, cell motility, and proliferation. Na⁺ currents were firstly discovered in 1949 by Hodgkin and Huxley in their study of action potentials in squid giant axon [1, 2]. This early work demonstrated that the resting membrane potential mostly depends on potassium permeability, whereas action potential is directly shaped by sodium permeability, which allows transient influx of Na⁺ to raise membrane potentials and is followed by rapid inactivation within milliseconds. From 1950s to 1970s, studies from many laboratories established conceptual models and equations conceptualizing sodium channel function [3].

1.1. Membrane potential, Nernst and Goldman equations

In a typical cell, sodium, potassium, chloride, and other membrane permeable ions are in unequal distribution across plasma membrane, **Figure 1A**. This unequal distribution and its resultant electrical gradient can be explained by Donnan equilibrium. For a specific ion, the electrical potential difference that exactly counterbalances diffusion due to the concentration difference is called the equilibrium potential for that specific ion. To use Na^+ as an example, at equilibrium, the chemical force moving Na^+ into the cell is balanced by the electrical force moving Na^+ out of the cell (**Figure 1B**).

For each ion, the equilibrium (or reversal) potential, E_{ion} , can be calculated by the Nernst equation (Eq. (1)), where R = gas constant, $8.135 \text{ J K}^{-1} \text{ mol}^{-1}$; T = temperature in K ($273 + \text{temp in } ^\circ\text{C}$); z = valency of ion ($\text{Na}^+ = 1$, $\text{Ca}^{2+} = 2$, and $\text{Cl}^- = -1$); F = Faraday's constant, $9.684 \times 10^4 \text{ C mol}^{-1}$. In a typical mammalian neuron with $[\text{Na}^+]$, $[\text{K}^+]$, and $[\text{Cl}^-]$ described in **Figure 1A**, based on Nernst equation, we can calculate $E_{\text{Na}} = 67 \text{ mV}$, $E_{\text{K}} = -83 \text{ mV}$, and $E_{\text{Cl}} = -61 \text{ mV}$. In cell resting state, the experimental measured membrane potential $E_m = -65 \text{ mV}$. As indicated in **Figure 2**, Na^+ has a tendency to flow into the cell due to $E_m < E_{\text{Na}}$, while K^+ flow out of the cell ($E_m > E_{\text{K}}$), and Cl^- near equilibrium ($E_m \approx E_{\text{Cl}}$). These concentration and electrical gradients are maintained by the dynamic equilibrium of ion channels and active ion transporters, most importantly by sodium pump (Na/K-ATPase).

$$E_{ion} = \frac{RT}{zF} \ln \frac{[\text{Ion}]_{out}}{[\text{Ion}]_{in}} \quad (1)$$

$$= 58.2 \text{ Log}_{10} \frac{[\text{Ion}]_{out}}{[\text{Ion}]_{in}} \quad (\text{when at } 20^\circ\text{C})$$

The whole cell membrane potential E_m can be calculated by all permeable ions' equilibrium potentials E_{ion} and their relative permeability P , which is described by Goldman-Hodgkin-Katz equation (GHK equation) (Eq. (2)). This equation explained the experimental finding that resting membrane potential is more depending on P_{K} , which is about 25-folds to P_{Na} .

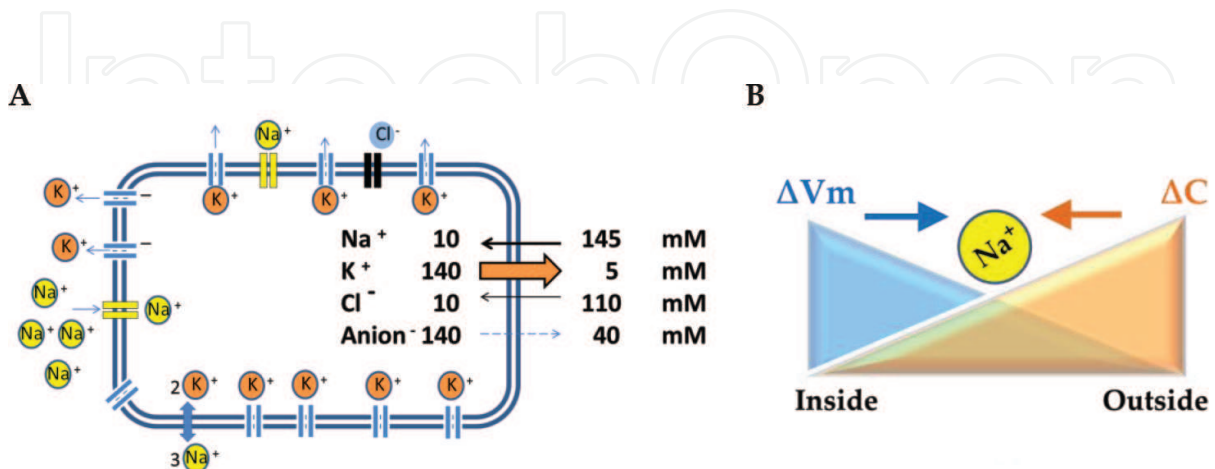


Figure 1. (A) Unequal distribution of ions in a typical mammalian neuron and (B) Donnan equilibrium scheme shows that the balance of concentration gradient and electrical gradient drives Na^+ movement toward inside or outside of the cell.

$$E_m = \frac{RT}{F} \ln \left(\frac{P_K[K^+]_{out} + P_{Na}[Na^+]_{out} + P_{Cl}[Cl^-]_{in}}{P_K[K^+]_{in} + P_{Na}[Na^+]_{in} + P_{Cl}[Cl^-]_{out}} \right) \quad (2)$$

$$= 58.2 \text{Log}_{10} \left(\frac{P_K[K^+]_{out} + P_{Na}[Na^+]_{out} + P_{Cl}[Cl^-]_{in}}{P_K[K^+]_{in} + P_{Na}[Na^+]_{in} + P_{Cl}[Cl^-]_{out}} \right) \quad (\text{when at } 20^\circ \text{C})$$

1.2. Hodgkin-Huxley model

The Hodgkin-Huxley model describes how action potentials in neurons are initiated and propagated [4]. Originally developed to fit action potential dynamics of squid giant axon, this model has been successfully applied to a wide range of neurons. It describes the electrical properties of excitable membranes as typical electrical circuit components. For instance, the cell membrane is modeled as a capacitor with capacitance (C_m) and ion channels are resistors with conductance of Na channel (g_{Na}), K channel (g_K), and leak channel (\bar{g}_L).

From Hodgkin-Huxley model, the total cell membrane current, I , can be calculated by Eq. (4), where membrane potential V_m , ion conductances g_{Na} and g_K , sodium activation variable m , sodium inactivation variable h , potassium activation variable n are variable functions of time, whereas E_{Na} , E_K , E_L , C_M , and \bar{g}_L are constants.

$$g_{Na} = \bar{g}_{Na} m^3 h_0 \left[1 - \exp \left(-\frac{t}{\tau_m} \right) \right]^3 \exp \left(-\frac{t}{\tau_h} \right) \quad (3)$$

$$I = C_m \frac{dV_m}{dt} + g_{Na} m^3 h (V_m - V_{Na}) + g_K n^4 (V_m - V_K) + \bar{g}_L (V_m - V_L) \quad (4)$$

Hodgkin-Huxley model provides a relatively simple and experimentally testable equation to deduce Na^+ conductance change with time and voltages (**Figure 2B**), and nerve action potential (**Figure 2C**). It also embodies the three key features of Nav channels: voltage-dependent activation (submillisecond scale), rapid inactivation (millisecond scale), and selective Na^+ conductance.

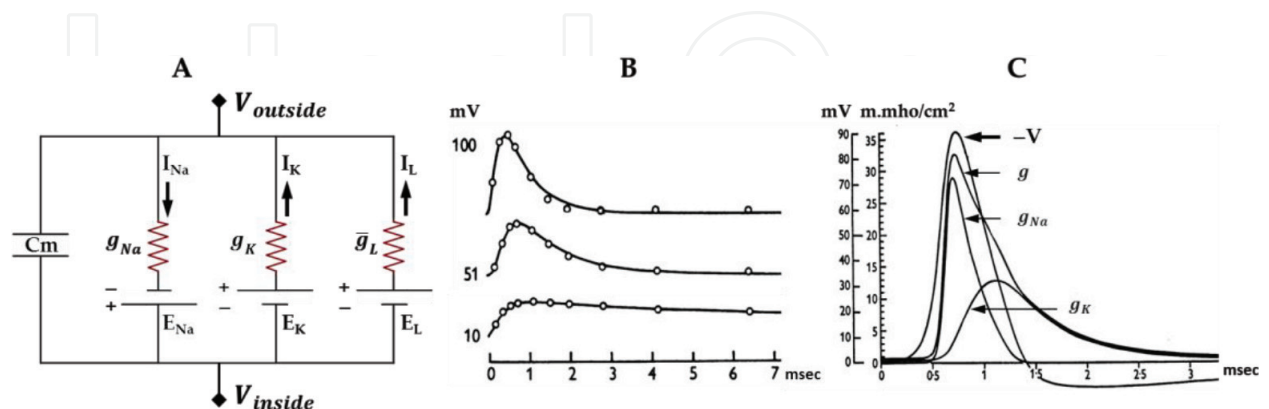


Figure 2. (A) Hodgkin-Huxley model, modified from Wikipedia. (B) Changes of sodium conductance associated with different depolarization voltages at 10, 51, and 100 mV. The circles are experimental sodium conductance, and the smooth curves are theoretical curves. (C) Calculated g_{Na} , g_K components of total membrane conductance (g) during propagated action potential ($-V$). Modified from [4].

1.3. History and basic concepts of electrophysiology

Electrophysiology was originated by Luigi Galvani in studying “animal electricity” in 1780s. In 1903, an extracellular recording technique, electrocardiography, was invented by Willem Einthoven (1924 Nobel Laureate); in 1952, intracellular recording technique was developed by Alan Hodgkin and Andrew Huxley (1963 Nobel Laureates); and in 1976, Erwin Neher and Bert Sackmann (1991 Noble Laureates) succeeded in measuring the ionic current of single channels in the cell membrane by developing patch clamp technique. These works were fundamental in revealing the physiological function of ion channels. Since then, the field of electrophysiology had undergone rapid evolution, especially after the introduction of automated patch clamp in the early 2000s.

Manual patch clamp technique employs glass microelectrode(s) with desired filling solution and tip diameter to perform either voltage or current clamp. For larger cells, such as *Xenopus* oocytes, two-electrode voltage clamp (TEVC) is performed using two electrodes: one to measure membrane potential and the other to apply the current, with each tip diameter $<1 \mu\text{m}$ resulting in 10–100 M Ω resistances. For most other circumstances, a single electrode with an open tip diameter 1–3 μm (1–3 M Ω resistances) is used for whole cells or small patches of cell membrane recording. A typical patch-clamp recording starts with cell attaching procedures including: placing glass tip next to a cell, using gentle suction, drawing a piece of the cell membrane to the microelectrode tip, and then letting glass tip to form a high-resistance seal with the cell membrane (ideally $>1\text{G}\Omega$, so-called “gigaseal”). By applying different following-up manipulations, the patch-clamp can be achieved in four configurations: cell-attached patch, whole-cell patch, inside-out patch, and outside-out patch, as shown in **Figure 3**.

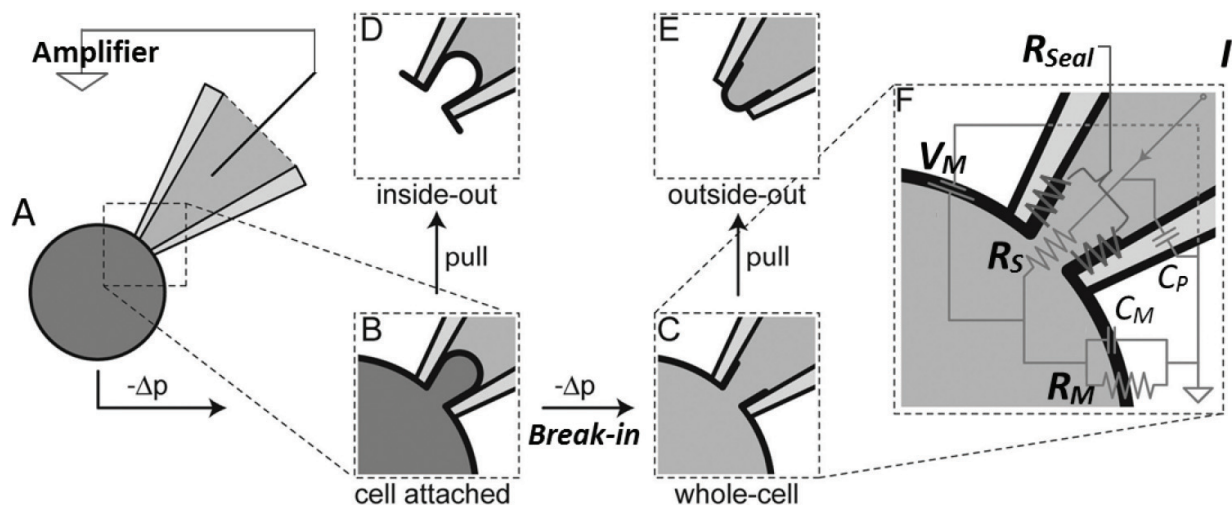


Figure 3. Manual patch clamp configurations and procedures. After a cell is approached by a pipette (A), a high-resistance seal is achieved through application of negative pressure, resulting in the cell-attached configuration (B). Further application of negative pressure ruptures the membrane, resulting in the whole-cell configuration, i.e., electrical contact with the inside of the cell (C). Inside-out and outside-out configurations are achieved by pulling the pipette away from the cell (D and E). (F) An equivalent electrical circuit of a cell in whole-cell configuration during acquisition of data. V_M = membrane potential, I = whole current, R_{Seal} = seal resistance, R_s = series resistance, R_M = membrane resistance, C_P = pipette capacitance, C_M = membrane capacitance. Modified from [5].

Many other electrophysiological techniques have been developed for various applications, including extracellular recordings such as electroencephalography (EEG), electrocardiography (ECG or EKG), and electromyography (EMG) for clinical diagnosis; artificial lipid bilayer recording for studying activities of reconstituted ion channel proteins; automated patch clamp recording to enable high-throughput recordings; and optogenetics to employ light to switch on and off ion channel activities. The technology evolution has brought the ion channel research and drug discovery to a new era, which will be discussed in later part of this chapter.

2. Nav channel general physiology

Nav channels were the first ion channel family discovered back in 1952 [1, 4] and cloned in 1984 [6]. Its pedigree spans across prokaryotic and eukaryotic kingdoms [7]. To date, ~500 Nav channels from bacteria (BacNavs) [8–10], and even more Nav channels from other species including fly [11], jellyfish [8], electric eel [12], cockroach [13], teleost fishes [8], and mammals have been cloned [14]. The BacNavs regulate the survival response to extreme pH, electrophiles, and hypoosmotic shock. Despite their markedly difference in physiology function, voltage dependence and kinetics, BacNavs share common features of mammalian Nav channels, thus serving as surrogates in the study of molecular evolution and channel architecture. Eukaryotic Navs display ultrafast kinetics, with milliseconds activation to inactivation, and high sodium ion selectivity, Na^+ (1): K^+ (0.14): Rb^+ (0.02): Cs^+ (0.005), which together enable them being responsible to initiate and transduce fast action potential firing in the vast electrical signaling pathways throughout the cardiovascular and nervous systems.

Nav family belongs to the voltage-gated ion channel (VGIC) superfamily, with less intrafamily variation comparing to the other two VGIC families, voltage-gated potassium channels (Kvs) and voltage-gated calcium channels (Cavs). The core functional unit of Nav channel is a tetrameric complex composed of four homologous domains (DI/II/III/IV), with each domain containing six transmembrane segments (S1–S6), an intracellular N-terminus and C-terminus. The first four transmembrane segments form a voltage-sensing domain (VSD) and the last two form the pore domain (PD). The central PD is responsible for ion-transduction through the structural top funnel, selectivity filter and gate, and all other domains are served as regulatory modlues for activation, fast and slow inactivation, albeit with different natures and structures.

Each eukaryotic Nav channel is composed of a single macromolecular α subunit (~2000 amino acid residues, ~260 kDa), forming a pseudoheterotetrameric core functional unit, in association with one or more auxiliary β subunits ($\beta 1$, $\beta 2$, $\beta 3$, and/or $\beta 4$, ~35 kDa) [15] (**Figure 4**). While the prokaryotic Navs are formed by four separate α subunit, similar to Kv channels, representing a simpler construction than eukaryotic Navs. A typical Nav channel has at least three distinct states, resting (closed), activated (open), inactivated (closed), which itself includes fast-inactivated (within milliseconds) and slow-inactivated (seconds), and recovering from inactivation (repriming), which is a period in which the channel is not available to open in response to a depolarization. Each Nav channel can be characterized by these different

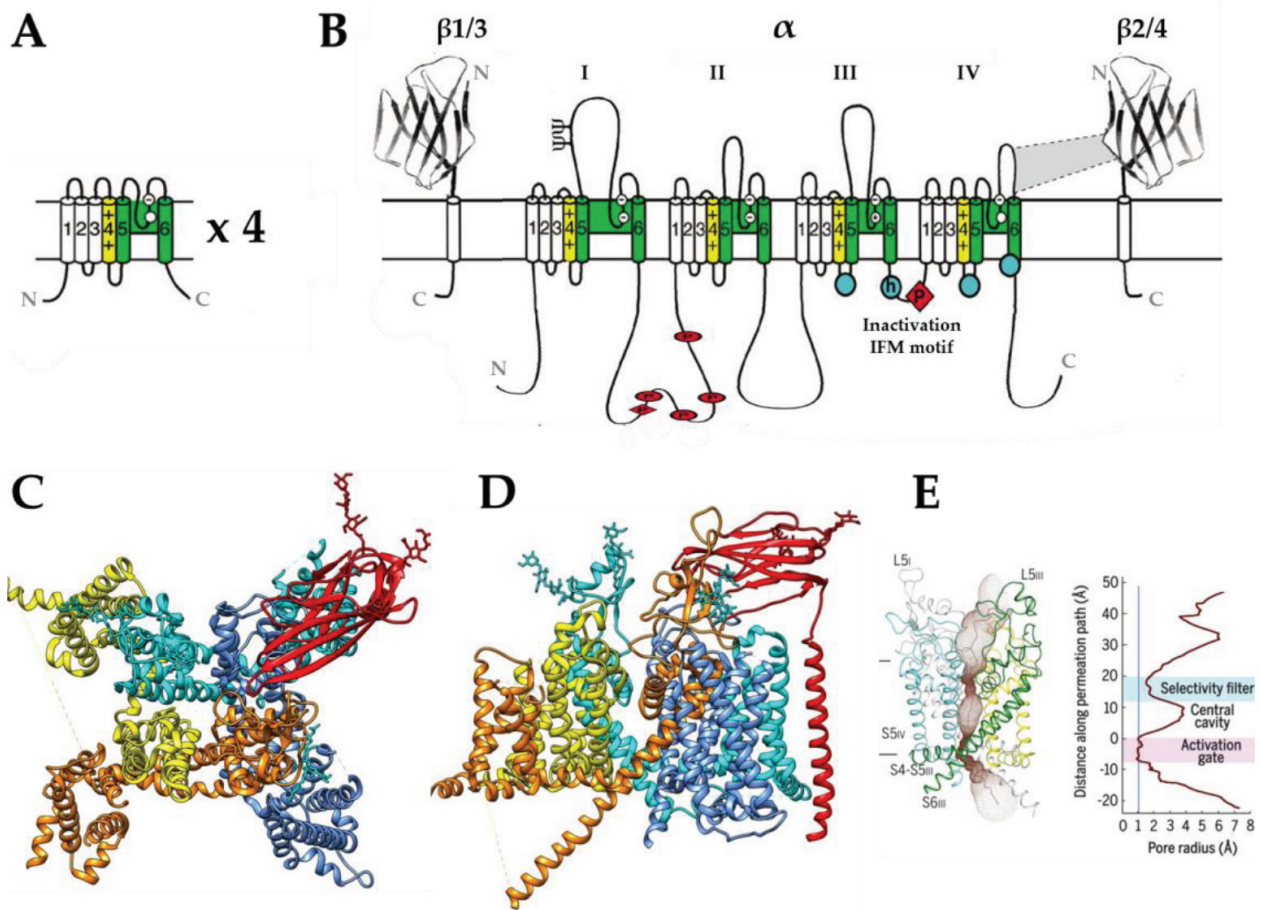


Figure 4. Structures of voltage-gated sodium channels. Modified from [12, 15]. (A) Schematic representation of BacNav. (B) Schematic representation of eukaryotic Navs. (C and D) The top and side views of the cryo-EM structure of EeNav1.4- $\beta 1$ complex (PDB 5XSY). The α -subunit domains DI-IV are colored orange, yellow, cyan, and blue, respectively, and the $\beta 1$ subunit is colored red. (E) The pore domain sodium permeation path including selectivity filter, central cavity, and intracellular activation gate are colored in brown and annotated with pore radius.

voltage-dependent biophysiological properties, and pharmacological properties according to its expression pattern and modulation.

In human, there are 9 Nav channels (Nav1.1-1.9), which are encoded by the genes SCN1A, SCN2A, SCN3A, SCN4A, SCN5A, SCN8A, SCN9A, SCN10A, and SCN11A, respectively. A tenth isoform, Nax, is considered as atypical, as it contains key difference in DI/III/IV S4 VSDs and DIII-IV inactivation linker, also it is activated by augmentation of extracellular sodium (over 150 mM) instead of voltage. Thus, Nax was classified as a different Nav subfamily (type 2) [16, 17]. Based on the timeline of gene cloning, each α subunit gene was assigned as SCN1A to SCN11A, and likewise, auxiliary β subunit genes were assigned as SCN1B to SCN4B, respectively (Table 1).

Due to their fundamental role in regulating central and peripheral nervous systems function, skeletal muscle contraction and heart rhythm, much of the early works on Navs involved characterizing their expression patterns, biophysiological properties, structure-function, and molecular pharmacology.

hNav isoform	Gene	Variant(s)	Human chromosome locus	UniProt	Homology*	TTX IC ₅₀ (nM)	Primary tissue location	Therapeutic relevance
Nine voltage-gated α subunits								
Nav1.1	SCN1A	3	2q24	P35498	90.0%	6	CNS, PNS	Epilepsy
Nav1.2	SCN2A	2	2q23–24	Q99250	90.8%	12	CNS, glia	Epilepsy, autism
Nav1.3	SCN3A	4	2q24	Q9NY46	90.0%	4	CNS, glia	Epilepsy
Nav1.4	SCN4A	1	17q23–25	P35499	76.8%	5	Skeletal muscle	Myotonia
Nav1.5	SCN5A	6	3p21	Q14524	79.4%	2000	Cardiac muscle	Cardiac rhythm disorders
Nav1.6	SCN8A	5	12q13	Q9UQD0	85.9%	1	CNS, PNS, glia	Ataxia, motor neuron disease
Nav1.7	SCN9A	4	2q24	Q15858	100%	4	Sensory neurons	Pain
Nav1.8	SCN10A	1	3p21–24	Q9Y5Y9	77.0%	60,000	Sensory neurons	Pain
Nav1.9	SCN11A	3	3p21–24	Q9UI33	70.4%	40,000	Sensory neurons	Pain
One nonvoltage-gated α subunits								
Navx	SCN7A**	1	2p21-23	Q01118	71.2%		PNS, DRG, epithelia	
Four β subunits								
Nav β 1	SCN1B	2	19q13	Q07699	100%		CNS, PNS, muscle	Epilepsy
Nav β 2	SCN2B	1	11q23	O60939	53.1%		CNS	
Nav β 3	SCN3B	1	11q23	Q9NY72	72.0%		CNS	
Nav β 4	SCN4B	3	11q23	Q8IWT1	57.9%		CNS, thyroid	

Data from Universal Protein Resource (UniProt, <http://www.uniprot.org>).

* α -subunit homology is calculated as the similarity between the most abundant isoform variant to Nav1.7 variant 3, which is the canonical sequence and position reference.

**SCN6A and SCN7A are orthologs of a single atypical Nav gene (SCN7A in mouse, the same gene was denoted as SCN6A in human).

Table 1. Human Nav channel subunits' gene information.

2.1. Genetic evolution and expression

Compared to Cav and Kv channel family, the rise of Nav family is relatively recent [18]. The study of intron/exon organization suggested that Navs were evolved from the similarly structured Cav channels. This is supported by the finding that the four domains of Navs have higher similarity to their corresponding domains in the Cav channels than to each other. The ancestral Navs and Caves genes might have evolved by two rounds of gene duplication, i.e., from an ancestral, single-domain Kv-like gene to a two-domain protein, then from a two-domain protein to a four-domain protein. This hypothesis is also in line with the observation that among the four domains of Navs, DI shares higher similarity with DIII, and DII shares higher similarity to DIV [19].

In choanoflagellate (the sister group of animals), the rapid long-distance communication among excitable cells is achieved at the emergence of Metazoa (represented by bilaterian animals and cnidarians) through the use of Nav channel [20, 21]. The gene organization, biophysical, and pharmacological properties of invertebrate sodium channels are largely similar to their mammalian counterparts, suggesting that the primordial Nav channels were established before the evolutionary separation of the invertebrates from the vertebrates, and evolution of Navs played a critical role in the emergence of nervous systems in animals [19, 22]. Of note, sodium selectivity might be acquired independently in BacNav and mammalian Nav channels as indicated by phylogenetic analysis [23]. Therefore, BacNav channels can serve as models for studying Navs structure function, but evolutionary variation should be taken into consideration.

Historically, the tissue distribution of mammalian Nav isoforms was obtained by methods such as quantitative PCR, expressed sequence tag (EST) profiling, and pharmacology study using isoform selective toxins. The more precise expression data were recently obtained by microarray [24, 25] and mRNA sequencing from Genotype-Tissue Expression (GTEx) project [26] (**Figure 5**). Now, we know that Nav1.1, Nav1.2, and Nav1.3 are predominantly expressed in central nervous system (CNS). Nav1.1 is the predominant channel in the caudal regions and the spinal cord, though relatively low-level expression of Nav1.1 has been shown in the peripheral nervous system (PNS). Nav1.2 is the highest expression isoform in the rostral regions. Nav1.3 peaks at birth but remains detectable at a lower level in adulthood. Interestingly, all of these CNS-enriched isoforms are sensitive to tetrodotoxin (TTX) at nanomolar concentrations, and their genes are clustered on chromosome 2 in both mice and humans.

Nav1.4 and Nav1.5 exhibit strikingly high-level expression in muscle and heart, respectively. More sensitive approaches have detected Nav1.5 in the piriform cortex and limbic regions of the brain but at relatively low level [27]. These two Nav isoforms can be distinguished from each other and from the CNS isoforms on the basis of toxin sensitivity. Adult skeletal muscle-enriched Nav1.4 is sensitive to TTX and μ conotoxin GIIIA at nanomolar concentrations, while the CNS-enriched channels are only sensitive to TTX, and heart-specific Nav1.5 is resistant to TTX. In addition, Nav1.4 is inhibited by nanomolar concentrations of μ conotoxin PIIIA, whereas Nav1.2 is approximately 15-fold less sensitive, and Nav1.7 is resistant [28–30].

Nav1.6 appears to be abundantly expressed in both PNS and CNS tissues. Nav1.7, Nav1.8, and Nav1.9 are primarily expressed in PNS, including nociceptive neurons, A β -fibers, C-fibers, and both large and small diameter dorsal root ganglion (DRG) [31]. This PNS-specific localization of Nav1.7, Nav1.8, and Nav1.9 make them attractive targets for developing isoform selective modulators to treat many PNS-related diseases and pathologic conditions.

2.2. Nav channel structure-function

The core functional unit of Nav channels is α subunit. Each α subtype is composed of a single polypeptide chain with \sim 2000 amino acid residues forming four pseudoheteromeric domains designated as DI to DIV. Nine α subunits' protein sequence homology is greater than 70% (**Table 1**). The structure complexity and high-sequence homology make it difficult to design

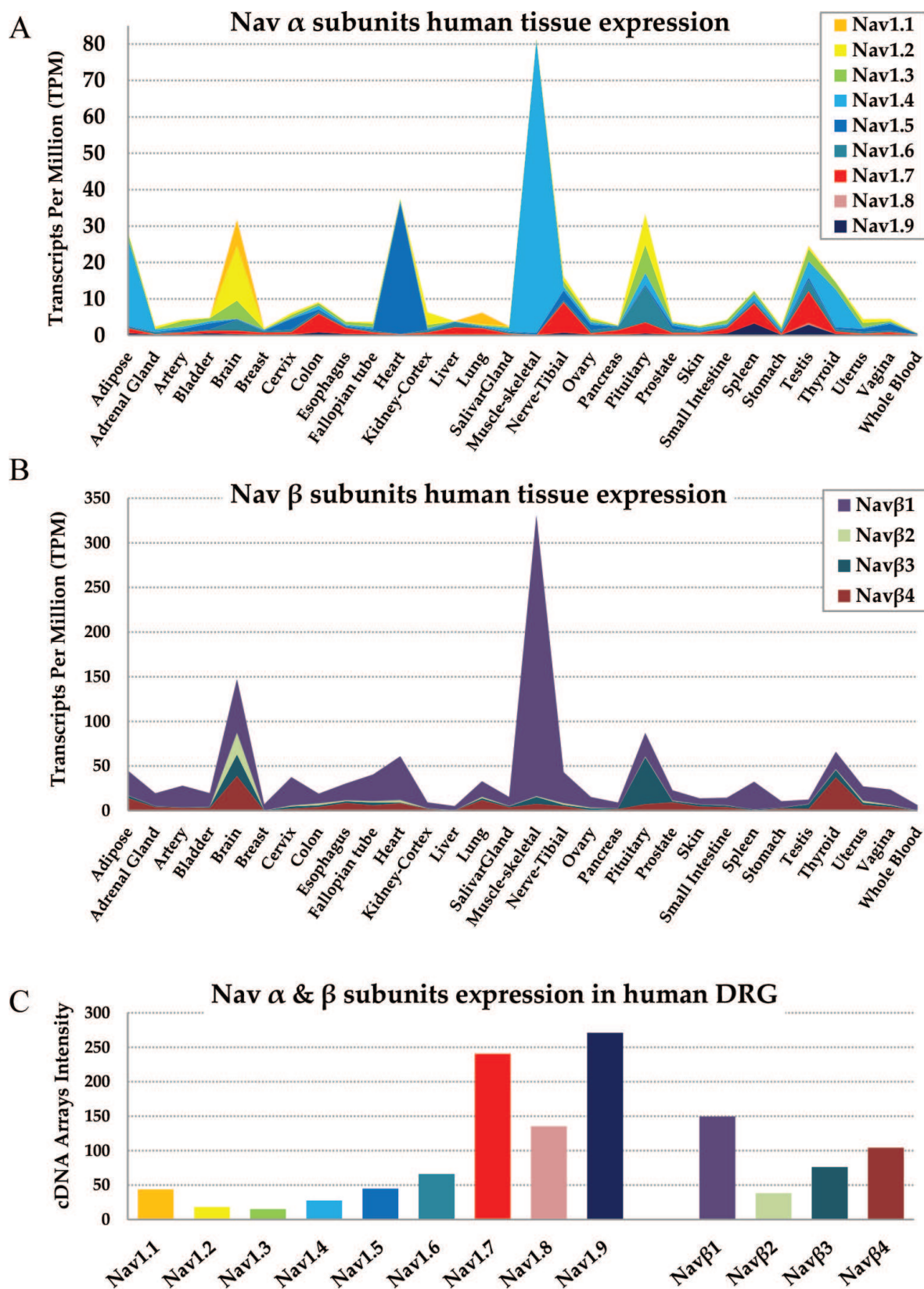


Figure 5. Sodium channel body atlas in human. (A and B) Human Nav α and β subunits tissue expression level from GTEx RNA-seq database (<https://www.gtexportal.org>). Gene expression level is presented as averaged tissue transcripts per million (TPM) value from 570 donors' 8555 samples. (C) Nav α and β subunits' expression level in human DRG. Gene expression level is presented as averaged cDNA microarray intensity number from 214 human DRG samples [56].

subtype-selective drugs. In 2011, the first X-ray crystal structure of bacterial *Arcobacter butzleri* Nav channels (NavAb) was determined [32]. Subsequently, structures for several BacNavs and a BacNav-human Nav chimeric channel have been resolved, representing closed [33, 34], open [34, 35], and potentially inactive states of the channels [36, 37]. In 2017, the first two eukaryotic Nav structures for American cockroach and electric eel (Ee) Nav1.4- β 1 complex were determined by using cryogenic electron microscopy (CryoEM) [12]. Findings from crystal and cryo-EM structures are mostly consistent, and collectively provided important insights into Nav channel structure-function and structure-based drug design.

Voltage-sensing domains (VSDs). The S1 to S4 segments form voltage-sensing domain. There are four VSDs in a sodium channel. Each VSD is featured by repetitively occurring positively charged Lys or Arg residues at every third position in S4. These charge clusters move toward the extracellular surface upon membrane depolarization and return to their resting positions upon membrane repolarization. Each VSD is connected to an intracellular S4-S5 linker, which transfers the movement of S4 segment to the central pore domain formed by S5-S6. Thus, the outward and inward movements of S4 result in channel opening and closing, respectively. Unlike homotetrameric Kvs and BacNavs, mammalian Nav channel's four VSDs possess distinctive sequence signature, conformation, and role in channel gating [12, 13]. For examples, the four VSDs have nonconserved intra- and extracellular loops, and the different charge clusters in S4, i.e., RRRR in DI, RRRRK in DII, KRRRR in DIII, and RRRRR in DIV. Also, the S2 in each VSD also makes asymmetric functional contributions to Nav channel activation and inactivation [38].

Pore domain (PD): the S5 to S6 segments from the four domains of the α subunits enclose the central pore of the channel. The extracellular linker connecting S5-S6 is defined as pore-loop (P-loop), which can be separated into two α helices named P1 and P2. The functional entities along the ion permeation pathway in PD include the selectivity filter (SF), the central cavity, and the intracellular activation gate, as shown in **Figure 4E**.

The outer vestibule and selectivity filter are formed in P-loop reentering membrane segments, designated as P1-SF-P2 funnel. Early study by comparing Navs with Cavs found that one residue, Asp/Glu/Lys/Ala (DEKA), at the corresponding locus in the middle of P1-P2 determines Na^+ selectivity [39]. Structure studies confirmed that the asymmetric selectivity filter vestibule is constituted by the side chains of the signature DEKA residues and the carbonyl oxygens atoms of the two preceding residues in each domain, Thr/Gln (DI), Cys/Gly (DII), Thr/Phe (DIII), and Thr/Ser (DIV). Mutational study identified an additional outer ring above the selectivity filter, Glu/Glu/Met/Asp (EEMD), which significantly interfered the tetrodotoxin (TTX) binding [40, 41]. The outer vestibule and SF structures were further discerned by using bacteria KcsA channel X-ray structure as template and guanidinium toxins (TTX and saxitoxin, STX), which successfully defined the first pharmacological relevant site on Nav channels, site 1 [42]. After that, local anesthetic binding site was determined within the four fenestrations in PD, each with distinct shape and size [13, 43]. From studying a group of activators, including batrachotoxin (BTX), veratridine (VTD), grayanotoxin (GTX), and aconitine (ACD), the neurotoxin site 2 was determined in the inner cavity of PD [44, 45].

Activation gate: the activation gate of Nav channels was originally predicted to be at the inner end of the pore based on the study of local anesthetics, which exhibit usage-dependent blockage [46, 47]. From thiol-modifying reagent accessibility study, a ~ 3.8 Å diameter constriction formed by a ring of conserved hydrophobic residues at the end of S6 (represented as DI-V440, DII-L795, DIII-I1287, DIV-I1590 in Nav1.4 and DI-Y405, DII-F960, DIII-F1449, DIV-F1752 in Nav1.7) was found to occlude only the pore at closed state but not at open state [48]. Recent cryo-EM structures confirmed that this activation gate is located at the cytoplasmic boundary level of the membrane [12]. Channelopathy study found that Nav1.7 DII S6 L955 deletion cause F960 side change conformational change in the activation gate. This mutation produces radial shift of the channel open at 25 mV more hyperpolarizing voltage, which renders hyperexcitability of DRG neurons to cause inherited erythromelalgia (IEM) [48].

Fast inactivation: while the channel opening is controlled by VSD and activation gate, the fast inactivation is regulated by a highly conserved Ile/Phe/Met (IFM) motif, which is localized in an intracellular loop connecting the domain DIII and DIV [49]. The IFM motif was originally discovered as a particle segment attached to the inner end of the pore. Study showed that pronase and N-bromoacetamide removed inactivation only when applied from intracellular side [50], and acetyl-KIFMK-amide peptides restored fast inactivation [51]. In the eukaryotic EeNav1.4- $\beta 1$ structure at open and resting states, the LFM motif (equivalent to IFM) in DIII-IV linker is plugged into the corner enclosed by the outer S4-S5 and inner S6 segments in DIII and DIV. Once the channel opens, the LFM motif acts as a hinged lid and folds into the intracellular mouth of the open pore to produce fast inactivation.

Slow inactivation: in contrast to fast inactivation (milliseconds scale), slow inactivation occurs in seconds during prolonged depolarization or rapid repetitive stimulations. Slow inactivation determines channel availability for action potential generation; thus, it endows neuronal tissues with memory of previous excitation, prevents excitation of skeletal muscle by mild hyperkalemia, and affects the conduction velocity and excitability of cardiac tissue. For the cardiac Nav1.5 channel, two putative proton sensor residuals in P-loop, C373 and H880, were responsible of tissue-acidification-induced slow inactivation underlying cardiac arrhythmia [52]. Other mutations, including DII S4-S5 linker L689I in Nav1.4, DII S6 Del-L955 in Nav1.7, have also been identified to impair slow inactivation, causing hyperkalemic periodic paralysis and inherited erythromelalgia, respectively [53, 54]. Voltage-clamp fluorimetry (VCF) study of Nav1.4 channels showed that that immobilization of DI and DII VSDs is involved in the development of slow inactivation, while DIII VSD is involved in the recovery from slow inactivation [55]. However, the structural basis for slow inactivation remains undefined.

2.3. Nav β subunits

In vertebrates, five Nav auxiliary β subunits, $\beta 1$, $\beta 1B$, $\beta 2$, $\beta 3$, and $\beta 4$, have been identified (SCN1B to SCN4B), with molecular weight ranging from 30 to 40 kD (**Table 1**) [57–60]. In invertebrates, auxiliary subunits such as tipE and Vssc β in drosophila bear no homology to vertebrate β subunits, suggesting a separate evolutionary pathway [61–63]. All β subunits comprise an amino terminal immunoglobulin (Ig) domain, a single transmembrane (TM)

segment, and an intracellular carboxyl-terminal, except for β 1B (previously named β 1A), which is a β 1 splice variant that lacks TM segment [64]. β 1 and β 3 interact with α subunit noncovalently, whereas β 2 and β 4 bind to the α subunit via a disulfide bond. All β isoforms are expressed in CNS, PNS, and cardiovascular systems, including excitable and nonexcitable cells, where they are part of the V-set immunoglobulin superfamily of cell adhesion molecules facilitating cell adhesion and cell migration. β 1 is highly expressed in skeletal and cardiac muscles, and the expression patterns of all β isoforms vary during development [65]. β subunits play broad role in modulating Nav function. They regulate expression and membrane trafficking of α subunits, modulate channel activation and inactivation, and interfere with toxin binding [66–68].

In 2017, the cryo-EM structure for EeNav1.4 in complex with the β 1 subunit was determined [12]. This structure provided a first glimpse into the interaction between α and β subunits. The β 1 subunit interacts with the α subunits as an ax, wherein its TM interacts with VSDIII within the membrane as the handle, while its Ig domain as the head interacts with DI-L5 and DIV-L6 extracellular loops and the intervening segment between DIII S1 and S2 (**Figure 4C and D**). Mutations in β subunits have been linked to many human diseases, including epilepsy, and cardiac arrhythmia, and sudden death syndromes. Although β subunit-specific drugs have not yet been developed, the Nav β subunit family remains a potential therapeutic target [68].

3. Channelopathy and therapeutic relevance

Nav channels are fundamentally important in a broad spectrum of physiological processes. Not surprisingly, genetic mutations of Nav channels result in many debilitating to severe phenotypes in CNS, PNS, cardiac, and neuromuscular systems. To date, at least ~50 human diseases have been attributed to aberrant activities of Nav channels; and hundreds of diseased related mutations of α and the β subunits have been identified. These mutations lead to channel dysfunctions called channelopathies (summarized in **Table 2**) and suggest the disease association of respective channels.

3.1. Pain

Nav1.7, 1.8, and 1.9 are highly expressed in sensory neurons. They control the excitability of nociceptive neurons, and thus are considered as therapeutic targets for pain relief [31, 71–74]. Among them, Nav1.7 was the first gene linked to human pain. In 2004, two missense mutations, I848T and L858H in SCN9A (Nav1.7), were associated with edema, redness, warmth, and bilateral pain in human inherited erythromelalgia (IEM) patients [75]. In 2006, three nonsense mutations, S459X, I767X, and W897X, were identified in congenital insensitivity to pain (CIP) patients [76]. Since then, additional gain-of-function mutations are associated with IEM, paroxysmal extreme pain disorder (PEPD), small fiber neuropathy (SFN), and additional loss-of-function mutations that are associated with CIP (**Figure 6**). The mechanism underlying these conditions was unraveled by characterizing biophysical properties of disease mutations

Isoform	Channelopathies	Discovered mutant number	Discovery publication number	
SCN1A	GEFS+2	Generalized epilepsy with febrile seizures plus 2	37	30
	EIEE6	Epileptic encephalopathy, early infantile, 6	317	41
	ICEGTC	Intractable childhood epilepsy with generalized tonic-clonic seizures	23	5
	FHM3	Migraine, familial hemiplegic, 3	5	4
	FEB3A	Febrile seizures, familial, 3A	2	2
SCN2A	BFIS3	Seizures, benign familial infantile 3	18	13
	EIEE11	Epileptic encephalopathy, early infantile, 11	50	21
	ASD	Autism spectrum disorders	16	1
SCN3A	CPE	Cryptogenic partial epilepsy	4	1
	ID	Intellectual disability	1	1
	AUTISM	Autism	2	1
	ADNSHL	Autosomal dominant nonsyndromic hearing loss	14	1
SCN4A	PMC	Paramyotonia congenita of von Eulenburg	16	16
	HOKPP2	Periodic paralysis hypokalemic 2	10	12
	HYPP	Periodic paralysis hyperkalemic	13	4
	NKPP	Periodic paralysis normokalemic	3	3
	MYOSCN4A	Myotonia SCN4A-related CMS16	14	13
	CMS16	Myasthenic syndrome, congenital, 16	3	3
	PAM	Potassium-aggravated myotonias	6	1
SCN5A	PFHB1A	Progressive familial heart block 1A	4	6
	LQT3	Long QT syndrome 3	123	30
	BRGDA1	Brugada syndrome 1	197	33
	SSS1	Sick sinus syndrome 1 VF1	2	3
	VF1	Familial paroxysmal ventricular fibrillation 1	1	1
	SIDS	Sudden infant death syndrome	2	1
	ATRST1	Atrial standstill 1	1	2
	CMD1E	Cardiomyopathy, dilated 1E	1	2
	ATFB10	Atrial fibrillation, familial, 10	9	2
	MEPPC	Multifocal ectopic Purkinje-related premature contractions	3	4
SCN8A	EIEE13	Epileptic encephalopathy, early infantile, 13	44	15
	BFIS5	Seizures, benign familial infantile, 5	1	2
SCN9A	IEM	Inherited erythralgia (primary erythralgia) pain	23	11
	CIP	Congenital insensitivity to pain	13	1
	PEPD	Paroxysmal extreme pain disorder	9	3
	GEFS+7	Generalized epilepsy with febrile seizures plus 7	2	1

Isoform	Channelopathies	Discovered mutant number	Discovery publication number
	FEB3B Febrile seizures, familial, 3B	2	1
	SFN Small fiber neuropathy	7	1
	DS (SMEI) Dravet syndrome (severe myoclonic epilepsy of infancy)	13	1
SCN10A	FEPS2 Episodic pain syndrome, familial, 2	2	1
	SFN Small fiber neuropathy	4	3
SCN11A	HSAN7 Neuropathy, hereditary sensory, and autonomic, 7	2	2
	FEPS3 Episodic pain syndrome, familial, 3	7	4
	SFN Small fiber neuropathy	4	4
SCN1B	ATFB13 Atrial fibrillation, familial, 13	2	1
	BRGDA5 Brugada syndrome 5	1	1
	EIEE52 Epileptic encephalopathy, early infantile, 52	2	2
	GEFS+1 Generalized epilepsy with febrile seizures plus 1	2	3
SCN2B	ATFB14 Atrial fibrillation, familial, 14	2	1
	BRGDA Brugada syndrome	1	1
SCN3B	ATFB16 Atrial fibrillation, familial, 16	4	2
	BRGDA7 Brugada syndrome 7	1	1
SCN4B	ATFB17 Atrial fibrillation, familial, 17	2	1
	LQT10 Long QT syndrome 10	1	1

Table 2. Nav α and β subunits' channelopathies data (updated in June, 2018 from database in <http://www.uniprot.org>).

[76] and nociceptor-specific Nav1.7 knockout [77]. Together, these studies have established that Nav1.7 is an essential and nonredundant requirement for nociception in humans.

While Nav1.7 is responsible for setting threshold for generation of action potentials, Nav1.8 and Nav1.9 contribute to the rising phase of action potentials in nociceptive neurons. Both channels are expressed in small-diameter DRG neurons, which include the C fibers that transmit nociceptive impulses [78]. Four gain-of-function Nav1.8 mutations (L554P, I1706V, A1304T, G1662S) have been identified, which lead to an increase in excitability in small-diameter neurons, underlying pain in small fiber neuropathy (SFN) [79–81]. In Nav1.9, gain-of-function mutations were recently reported to be associated with pain, albeit with opposing effects [82]. So far, naturally occurring loss-of-function mutations of Nav1.8 and Nav1.9 are yet to be described in humans; Nav1.8 and 1.9 are clearly important in the pain pathology and worth exploring as potential pain targets.

3.2. Epilepsy

Nav channel dysfunction is central to the pathophysiology of epileptic seizures, and many of the most widely used antiepileptic drugs, including phenytoin, carbamazepine, and lamotrigine,

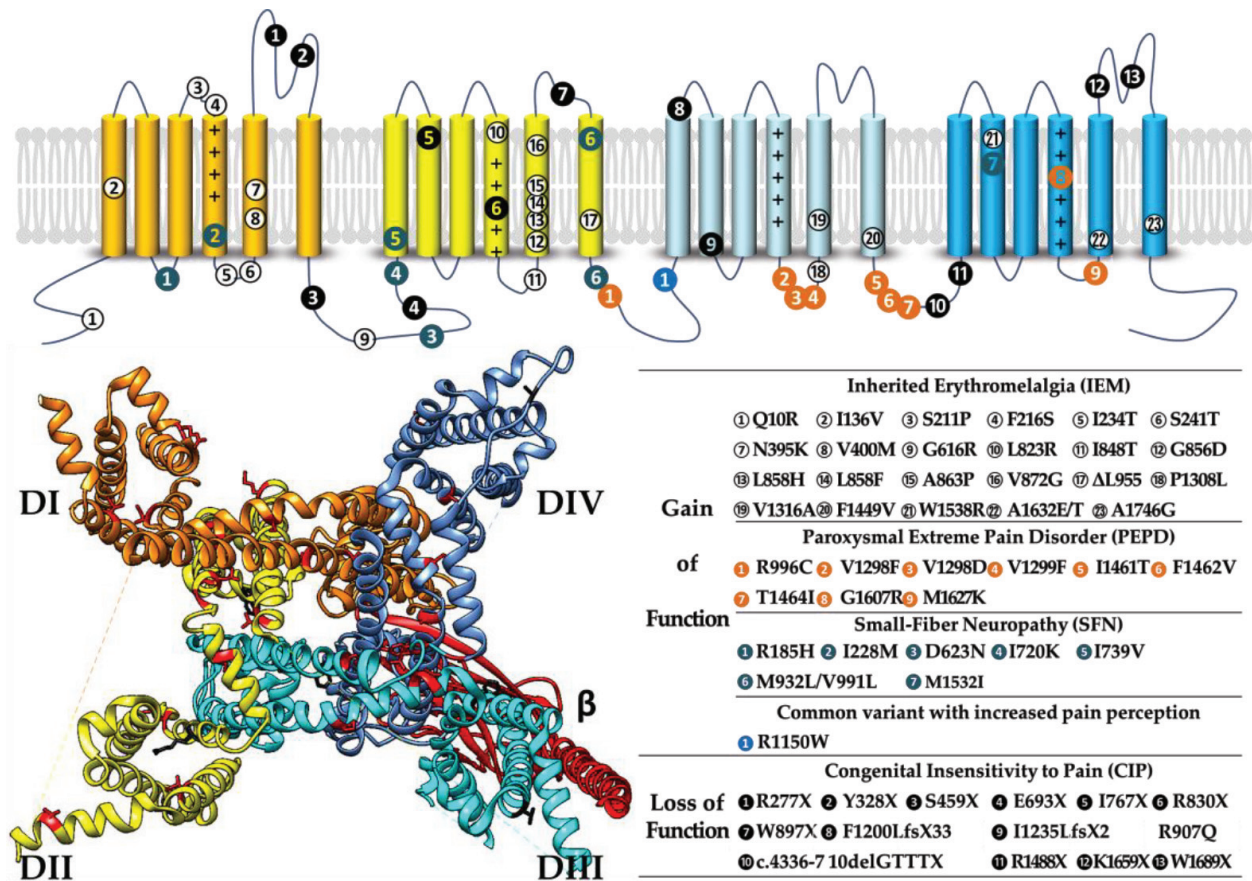


Figure 6. Amino acid locations of Nav1.7 disease-related mutations on the Nav1.7 structure model. Modified from [12, 31, 69–71].

are Nav inhibitors. Many types of general epilepsy are resulted from mutations primarily in Nav1.1, and also in other Nav α isoforms, including Nav1.2, Nav1.3, Nav1.6, Nav1.7, and Nav β 1. GEFS+ type 1 results from Nav β 1 mutation C387G, which destroys extracellular immunoglobulin domain and thus indirectly decreases rate of channel inactivation [83]. GEFS+ type 2 results from Nav1.1 mutations, such as T875 M (in DII-S4) and R1648H (in DIV-S4), which decrease Nav1.1 inactivation rate directly [84]. Worth noting, some epilepsy-associated Nav1.2 and Nav1.6 mutations cause a gain-of-function when characterized in transfected cells [85, 86]. Better understanding of clinical genetics and channel structure-function will facilitate the drug development for Nav-associated neurological diseases.

3.3. Cardiac arrhythmias

Mutations of Nav1.5 have been linked to long QT syndrome (LQTS). Recent study suggests that even modest depression of Nav1.5 expression may promote pathologic cardiac remodeling and progression of heart failure [87]. Since the first LQT-related Nav1.5 mutation being discovered in 1995 [88], more than a hundred Nav1.5 mutations that associate with distinct cardiac rhythm disorders, such as LQT syndrome subtype 3, Brugada syndrome, and cardiac conduction disease, have been identified [89]. These Nav1.5 mutations are spread out the whole protein. Most Nav1.5 mutations change biophysical property by increasing persistent

Na⁺ current or gain-of-function, while in Brugada syndrome and cardiac conduction disease, most of the mutations are missense loss-of-function mutations. Because many mutations produce overlapping clinical phenotypes, it is crucial to understand genotype-phenotype correlations in Nav1.5 channelopathies for drug development.

3.4. Neuromuscular diseases

Mutations of Nav1.4 channel are associated with inherited neuromuscular diseases. For example, the M1592V mutation causes hyperkalemic periodic paralysis (HYPP), in which increased levels of serum potassium lead to muscle hypoexcitability and paralysis; the R1448C mutation causes paramyotonia congenita (PMC), which is induced by cold and aggravated by increased muscle activity; and the G1306A mutation causes potassium-aggravated myotonias (PAM). These mutations affect either voltage-dependent activation or inactivation of Nav1.4, and are inherited in an autosomal dominant manner [90]. In contrast, most Nav1.6 mutations are recessive. An allelic mutation A107T in DIII S4-S5 caused ataxic phenotype by shifting Nav1.6 activation and inactivation to about 14 mV in the depolarizing direction, suggesting Nav1.6 is required for the complex spiking of cerebellar Purkinje cells and for persistent sodium current in several classes of neurons [91–93].

4. Nav modulation with small and large molecules

Nav channels have long been recognized as targets for treating pain, neurological disorders, and cardiac arrhythmias. In nature, Nav channels are the molecular targets of a broad range of neurotoxins including tetrodotoxin (TTX), saxitoxin (STX), veratridine (VTD), and batrachotoxin (BTX) from marine bacteria and plants, as well as peptide toxins such as ProToxin (ProTX), Huwentoxin (HwTX and α -ScTXs) from the venoms of scorpions, spiders, sea anemones, and cone snails. Additionally, many Nav-targeting drugs have been developed, including local anesthesia (LA), antiarrhythmics (e.g., lidocaine, mexiletine), anticonvulsants (e.g., carbamazepine), and antidepressants (e.g., amitriptyline). In general, these drugs do not have subtype selectivity and have small therapeutic index. Recently, two series of highly isoform-selective compounds, aryl sulfonamides for Nav1.7 and phenyl imidazole for Nav1.8, have been reported [94, 95]. Besides small molecules, monoclonal antibody has also been proposed as an alternative strategy. Nonetheless, due to the high-sequence homology among all Nav isoforms, subtype selective targeting remains a challenge.

All nature or synthesized small and large modulators for Nav channels can be classified as pore blockers or gating modifiers. Pore blockers (e.g., TTX) physically occlude the pore, thereby inhibiting channel conductance. Often the blockade is tonic, or independent of states of the channels. Gating modifiers (aryl sulfonamides as example) preferentially modify activated or inactivated states, thus reducing currents progressively with increased stimulation duration and frequency.

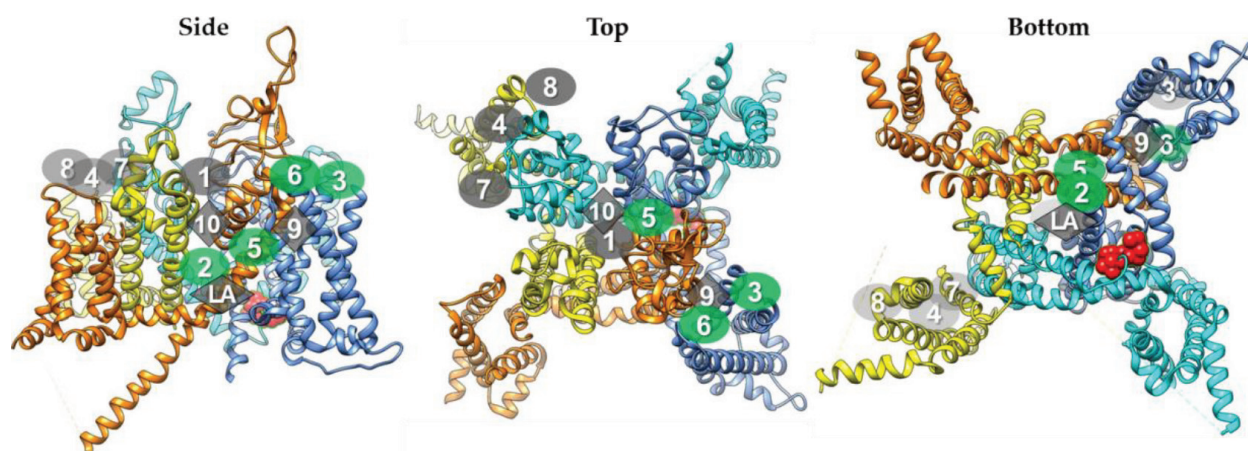


Figure 7. Nav channel structural topology with drug binding sites. Domain DI/II/III/IV is colored orange, yellow, cyan, and blue, respectively. The IFM fast inactivation gate is shown in red sphere format. All currently identified eight Nav binding sites are labeled corresponding to its visibility. Binding sites leading to channel activation are in green, and binding sites leading to channel blockage are in gray. Seven natural toxin binding sites are labeled with oval, while local anesthetic, aryl sulfonamide, and phenyl imidazole binding sites are labeled with diamonds.

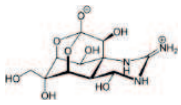
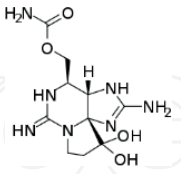
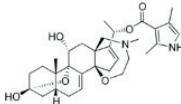
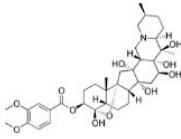
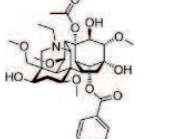
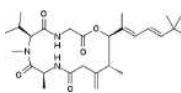
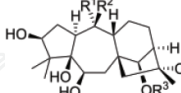
Based on their drug binding sites, Nav inhibitors can be classified into different groups (**Figure 7** and **Table 3**).

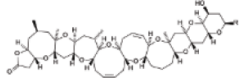
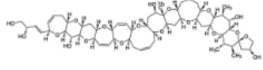
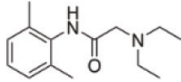
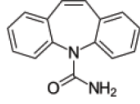
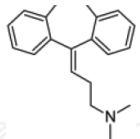
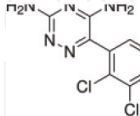
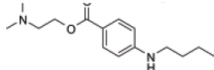
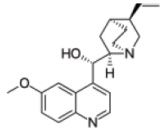
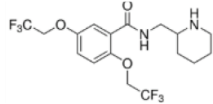
Site 1: extracellular pore blocker. This site is formed by the four P-loops and represents the binding site of two known groups of pore blockers, including small molecular guanidinium toxins from marine bacteria (TTX and STX), and 17–25 amino acids' peptide μ -conotoxins from marine cone snail toxins [96–98]. These toxins physically plug the pore and thereby inhibit the sodium conductance.

Site 2: intracellular pore gating activator (state dependent). The binding site is the fenestration site formed between DI-S6 and DIV-S6, which binds to many small lipid-soluble toxins including batrachotoxin (BTX) from frog, antillatoxin (ATX) from marine species, and veratridine (VTD), aconitine (ACT), and grayanotoxin (GTX) from plants. These modulators facilitate channel activation or prevent inactivation, thereby increasing channel conductance. They often have much higher affinity to the open and inactivated states of Nav channel as the binding fenestration exposed.

Site 3: extracellular gating activator. The binding site is localized in the DIV S3-S4 extracellular loop for two groups of peptide toxin activators: scorpion α -toxins (α -ScTx) and sea. Upon binding, these modulators prevent the movement of DIV-S4, thus inhibiting transition to fast inactivation.

Site 4: extracellular gating blocker. The binding site is the DII S1-S2 and S3-S4 extracellular loop, which binds to four groups of peptide toxin blockers, including β -scorpion toxins (β -ScTx), β -spider toxins, μ O-conotoxins, and ι -conotoxins. In general, these toxins block the DII-VSD conformational change and shift the voltage dependence of activation toward more hyperpolarized potentials, though the structural-based mechanism of action is not clear.

Binding site	Molecule group	Effect and application	Molecule examples	Structure or peptide PDB	Reference	
Site 1. DI-IV P-loop	Marine bacteria toxin	Block Na ⁺ conduction	Tetrodotoxin (TTX)		[96]	
			Saxitoxin (STX)		[97]	
			μ -Conotoxin	KIIIA	17 aa, 2LXG	[98]
			PIIIA, PIIIB	22 aa, 1R9I	[98]	
			GIIIA, GIIIB	23 aa, 1TCG	[98]	
			BuIIIB	25 aa, 2LOC	[98]	
Site 2. DI-DIV S6	Small lipid-soluble toxins	Prevent inactivation Nav agonist	Batrachotoxin (BTX)		[102]	
			Veratridine (VTD)		[103]	
			Aconitine (ACT)		[104]	
			Antillatoxin (ATX)		[105]	
			Grayanotoxin (GTX)		[106]	
			Site 3. DIV-S3-S4	α -Scorpion toxins	Prevent inactivation Nav agonist	Aah 2
LqhaIT	65 aa, 1LQH	[107]				
LqhIT2	62 aa, 2I6I	[107]				
BMK MI	64 aa, 1SN1	[107]				
Sea anemone toxins	Type I: ATXI, etc.	46 aa, 1ATX		[108]		
	Type II: Rp2, etc.	48 aa		[108]		
	Type III: ATX3, etc.	27 aa, 1ANS		[108]		
	Site 4. DII S3-S4	β -Scorpion toxins (β -ScTxS)		Prevent activation	Cn2	67 aa, 1CN2

Binding site	Molecule group	Effect and application	Molecule examples	Structure or peptide PDB	Reference
			Ts1 (=Ts7, TsVII, Tsγ)	61 aa, 1B7D	[109]
			Bj-xtrIT	77 aa, 1BCG	[109]
			LqhIT2	62 aa, 2I61	[109]
	β-Spider toxins		ProTXI	35 aa, 2M9L	[110]
			ProTX II	30 aa, 2N9T	[110]
			HwTX-IV	35 aa, 1MB6	[111]
			Magi 5	29 aa, 2GX1	[112]
	μO-conotoxins		μO-MrVIB	31 aa, 1RMK	[113]
	ι-conotoxins		ι-RxIA	38 aa, 2JTU	[113]
Site 5. DIV S6	Cyclic polyethers (dinoflagellate toxin)	Prevent inactivation, Nav agonist	Brevetoxins (PbTx)		[114]
			Ciguatoxins (CTX1)		[101]
Site 6. DIV S4	Cysteine knot 3 disulfide bridges	Conotoxins Nav agonist	δ-TxVIA	27 aa, 1FU3	[115]
			δ-EVIA	33 aa, 1G1P	[113]
Site 7. (LA) DIV S6	Local anesthetics	Local anesthetics Class Ib antiarrhythmic Neoropathic pain	Lidocaine		[116]
	State-dependent nonselective Na ⁺ conduction blockers	Antidepressant	Carbamazepine		[116]
		Antidepressant	Amitriptyline		[117]
		Anticonvulsant	Lamotrigine		[118]
		Local anesthetic	Tetracaine		[119]
		Class Ia antiarrhythmic	Quinidine		[120]
		Class Ic antiarrhythmic	Flecainide		[121]

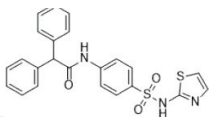
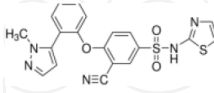
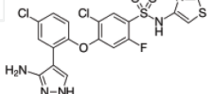
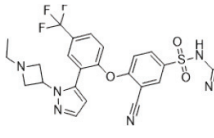
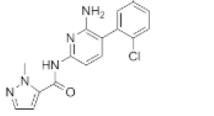
Binding site	Molecule group	Effect and application	Molecule examples	Structure or peptide PDB	Reference
Site 8. DII S2	Cysteine knot	Conotoxins Nav antagonist	μ O \S -GVIIJ	35 aa, 2N8H	[100]
Site 9. DIV S4	Aryl sulfonamides	Nav1.7 selective blockers	ICA-121431 (Icagen)		[101]
			PF-04856264 (Pfizer)		[101]
			PF-05089771 (Pfizer)		[122]
			GX-936		[123]
			Site 10	Phenyl imidazole	Nav1.8 selective blockers
PF-04531083 (Pfizer)		[95]			

Table 3. Small molecules and toxin modulators for Nav channels.

Site 5: intracellular pore gating activator (state dependent). The fenestration site between DI-S6 and DIV-S5 binds two classes of cyclic polyether toxins from dinoflagellate: brevetoxins (PbTx) and ciguatoxins (CTX). These modulators have higher affinity to activated channel. Upon binding, they shift the activation and inactivation both to more hyperpolarizing voltage, thus keeping the channel hyperactive.

Site 6: extracellular gating activator. The DIV-S4 fenestration binds to δ -conotoxins causing similar effects as site 3 toxins by slowing or inhibiting inactivation. Although sites 6 and 3 are structurally close to each other, however, the two categories activators do not compete with each other [99]. Site 6 activators trap DIV-S4 in outward conformation, thus leading to a persistent activation and prolongation of action potential.

Site 7: local anesthetic (LA) binding site. The inner cavity of channel pore, consisting of amino acid residues in S6 of DI, DIII, and DIV, forms the LA binding site. The LA binding site is highly conserved across Nav channels and accounts for the lack of subtype selectivity for most clinically used sodium channel blockers.

Site 8: extracellular gating blocker. The site was identified by studying a class of cone snail $\mu\text{O}\xi$ -conotoxins blockers, such as $\mu\text{O}\xi$ -GVIIJ. The putative binding site is close to a cysteine near DII P-loop (C910 in rNav1.2), which is responsible of the antagonist effect [100].

Site 9: aryl sulfonamide site. The unique Nav1.7 VSD4 binding site for the new series of aryl sulfonamide compounds, such as ICA-121431, PF-04856264 [101].

Site 10: phenyl imidazole site. The unique fenestration-selectivity filter site in Nav1.8 for the new series of phenyl imidazole compounds, such as A-803467, PF-04531083 [95].

5. Concluding remarks

Voltage-gated sodium channels play essential roles in physiological function, and historically, sodium channel blockers have been developed as local anesthetics and anticonvulsants. However, these early generation of sodium channel drugs were developed decades ago without the exact understanding of their molecular targets and mechanisms of action; their general lack of on-target potency and off-target selectivity renders narrow therapeutic windows. In recent years, several scientific frontiers have been rapidly evolving. First, the physiological functions of each sodium channel have been determined. Second, their associations to human diseases have been revealed in the form of “channelopathies.” Often both gain-of-function and loss-of-function mutations have been linked to human diseases, therefore pinpointing exactly the molecular targets. Third, the structural determination of sodium channels provides opportunities for structural-based drug design. Together, these progresses have ushered in a new, exciting era of sodium channel drug discovery.

Acknowledgements

We gratefully acknowledge contributions from Genentech Inc. to support this publication.

Conflict of interest

The authors are all employees of Genentech Inc. (a Roche Group Company) and declare no financial and conflict of interest in this chapter.

Notes/thanks/other declarations

N/a.

Author details

Tianbo Li* and Jun Chen

*Address all correspondence to: li.tianbo@gene.com

Department of Biochemical and Cellular Pharmacology, Genentech Inc., South San Francisco, California, USA

References

- [1] Hodgkin AL, Huxley AF. Currents carried by sodium and potassium ions through the membrane of the giant axon of *Loligo*. *The Journal of Physiology*. 1952;**6**:449-472
- [2] Hodgkin AL, Katz B. The effect of sodium ions on the electrical activity of the giant axon of the squid. *The Journal of Physiology*. 1949;**8**:37-77
- [3] Armstrong CM. Sodium channels and gating currents. *Physiological Reviews*. 1981;**61**:644-683. DOI: 10.1152/physrev.1981.61.3.644
- [4] Hodgkin AL, Huxley AF. A quantitative description of membrane current and its application to conduction and excitation in nerve. *The Journal of Physiology*. 1952;**117**:500-544
- [5] Pihl J, Sinclair J, Karlsson M, Orwar O. Microfluidics for cell-based assays. *Materials Today*. 2005;**8**:46-51. DOI: 10.1016/S1369-7021(05)71224-4
- [6] Noda M, Shimizu S, Tanabe T, Takai T, Kayano T, Ikeda T, Takahashi H, Nakayama H, Kanaoka Y, Minamino N, Kangawa K, Matsuo H, Raftery MA, Hirose T, Inayama S, Hayashida H, Miyata T, Numa S. Primary structure of *Electrophorus electricus* sodium channel deduced from cDNA sequence. *Nature*. 1984;**312**:121-127. DOI: 10.1038/312121a0
- [7] Hille B. *Ion Channels of Excitable Membranes*. 3rd ed. Sunderland, MA: Sinauer Associates Inc.; 2001
- [8] Spafford JD, Spencer AN, Gallin WJ. A putative voltage-gated sodium channel α subunit (PpSCN1) from the hydrozoan jellyfish, *Polyorchis penicillatus*: Structural comparisons and evolutionary considerations. *Biochemical and Biophysical Research Communications*. 1998;**244**:772-780. DOI: 10.1006/bbrc.1998.8332
- [9] Ren D, Navarro B, Xu H, Yue L, Shi Q, Clapham DE. A prokaryotic voltage-gated sodium channel. *Science*. 2001;**294**:2372-2375. DOI: 10.1126/science.1065635
- [10] Payandeh J, Minor DL. Bacterial voltage-gated sodium channels (BacNavs) from the soil, sea, and salt lakes enlighten molecular mechanisms of electrical signaling and pharmacology in the brain and heart. *Journal of Molecular Biology*. 2014;**427**:3-30. DOI: 10.1016/j.jmb.2014.08.010

- [11] Knipple DC, Doyle KE, Marsella-Herrick PA, Soderlund DM. Tight genetic linkage between the *kdr* insecticide resistance trait and a voltage-sensitive sodium channel gene in the house fly. *Proceedings of the National Academy of Sciences of the United States of America*. 1994;**91**:2483-2487
- [12] Yan Z, Zhou Q, Wang L, Wu J, Zhao Y, Huang G, Peng W, Shen H, Lei J, Yan N. Structure of the Nav1.4- β 1 complex from electric eel. *Cell*. 2017;**170**:470-482.e11. DOI: 10.1016/j.cell.2017.06.039
- [13] Shen H, Zhou Q, Pan X, Li Z, Wu J, Yan N. Structure of a eukaryotic voltage-gated sodium channel at near-atomic resolution. *Science*. 2017;**355**:eaal4326. DOI: 10.1126/science.aal4326
- [14] Goldin AL. Resurgence of sodium channel research. *Annual Review of Physiology*. 2001; **63**:871-894. DOI: 10.1146/annurev.physiol.63.1.871
- [15] Yu FH, Catterall WA. Overview of the voltage-gated sodium channel family. *Genome Biology*. 2003;**4**:207
- [16] Noda M, Hiyama TY. The Nav Channel. What it is and what it does. *Neuroscience*. 2015; **21**:399-412. DOI: 10.1177/1073858414541009
- [17] George AL, Knittle TJ, Tamkun MM. Molecular cloning of an atypical voltage-gated sodium channel expressed in human heart and uterus: Evidence for a distinct gene family. *Proceedings of the National Academy of Sciences of the United States of America*. 1992; **89**:4893-4897
- [18] Strong M, Chandy KG, Gutman GA. Molecular evolution of voltage-sensitive ion channel genes: On the origins of electrical excitability. *Molecular Biology and Evolution*. 1993; **10**:221-242. DOI: 10.1093/oxfordjournals.molbev.a039986
- [19] Plummer NW, Meisler MH. Evolution and diversity of mammalian sodium channel genes. *Genomics*. 1999;**57**:323-331. DOI: 10.1006/GENO.1998.5735
- [20] Liebeskind BJ, Hillis DM, Zakon HH. Evolution of sodium channels predates the origin of nervous systems in animals. *Proceedings of the National Academy of Sciences of the United States of America*. 2011;**108**:9154-9159. DOI: 10.1073/pnas.1106363108
- [21] Moran Y, Barzilai MG, Liebeskind BJ, Zakon HH. Evolution of voltage-gated ion channels at the emergence of Metazoa. *The Journal of Experimental Biology*. 2015;**218**:515-525. DOI: 10.1242/jeb.110270
- [22] Lopreato GF, Lu Y, Southwell A, Atkinson NS, Hillis DM, Wilcox TP, Zakon HH. Evolution and divergence of sodium channel genes in vertebrates. *Proceedings of the National Academy of Sciences*. 2001;**98**:7588-7592. DOI: 10.1073/pnas.131171798
- [23] Liebeskind BJ, Hillis DM, Zakon HH. Independent acquisition of sodium selectivity in bacterial and animal sodium channels. *Current Biology*. 2013;**23**:R948-R949. DOI: 10.1016/J.CUB.2013.09.025

- [24] Raymond CK, Castle J, Garrett-Engele P, Armour CD, Kan Z, Tsinoremas N, Johnson JM. Expression of alternatively spliced sodium channel alpha-subunit genes. Unique splicing patterns are observed in dorsal root ganglia. *Journal of Biological Chemistry*. 2004;**279**: 46234-46241. DOI: 10.1074/jbc.M406387200
- [25] Parisien M, Khoury S, Chabot-Doré A-J, Sotocinal SG, Slade GD, Smith SB, Fillingim RB, Ohrbach R, Greenspan JD, Maixner W, Mogil JS, Belfer I, Diatchenko L. Effect of human genetic variability on gene expression in dorsal root ganglia and association with pain phenotypes. *Cell Reports*. 2017;**19**:1940-1952. DOI: 10.1016/j.celrep.2017.05.018
- [26] Ardlie KG, Deluca DS, Segre AV, Sullivan TJ, Young TR, Gelfand ET, Trowbridge CA, Maller JB, Tukiainen T, Lek M, Ward LD, Kheradpour P, Iriarte B, Meng Y, Palmer CD, Esko T, Winckler W, Hirschhorn JN, Kellis M, MacArthur DG, Getz G, Shabalin AA, Li G, Zhou Y-H, Nobel AB, Rusyn I, Wright FA, Lappalainen T, Ferreira PG, Ongen H, Rivas MA, Battle A, Mostafavi S, Monlong J, Sammeth M, Mele M, Reverter F, Goldmann JM, Koller D, Guigo R, McCarthy MI, Dermitzakis ET, Gamazon ER, Im HK, Konkashbaev A, Nicolae DL, Cox NJ, Flutre T, Wen X, Stephens M, Pritchard JK, Tu Z, Zhang B, Huang T, Long Q, Lin L, Yang J, Zhu J, Liu J, Brown A, Mestichelli B, Tidwell D, Lo E, Salvatore M, Shad S, Thomas JA, Lonsdale JT, Moser MT, Gillard BM, Karasik E, Ramsey K, Choi C, Foster BA, Syron J, Fleming J, Magazine H, Hasz R, Walters GD, Bridge JP, Miklos M, Sullivan S, Barker LK, Traino HM, Mosavel M, Siminoff LA, Valley DR, Rohrer DC, Jewell SD, Branton PA, Sobin LH, Barcus M, Qi L, McLean J, Hariharan P, Um KS, Wu S, Tabor D, Shive C, Smith AM, Buia SA, Undale AH, Robinson KL, Roche N, Valentino KM, Britton A, Burges R, Bradbury D, Hambright KW, Seleski J, Korzeniewski GE, Erickson K, Marcus Y, Tejada J, Taherian M, Lu C, Basile M, Mash DC, Volpi S, Struewing JP, Temple GF, Boyer J, Colantuoni D, Little R, Koester S, Carithers LJ, Moore HM, Guan P, Compton C, Sawyer SJ, Demchok JP, Vaught JB, Rabiner CA, Lockhart NC, Ardlie KG, Getz G, Wright FA, Kellis M, Volpi S, Dermitzakis ET. The genotype-tissue expression (GTEx) pilot analysis: Multitissue gene regulation in humans. *Science (80-)*. 2015;**348**: 648-660. DOI: 10.1126/science.1262110
- [27] Hartmann HA, Colom LV, Sutherland ML, Noebels JL. Selective localization of cardiac SCN5A sodium channels in limbic regions of rat brain. *Nature Neuroscience*. 1999;**2**:593-595. DOI: 10.1038/10147
- [28] Safo P, Rosenbaum T, Shcherbatko A, Choi DY, Han E, Toledo-Aral JJ, Olivera BM, Brehm P, Mandel G. Distinction among neuronal subtypes of voltage-activated sodium channels by mu-conotoxin PIIIA. *The Journal of Neuroscience*. 2000;**20**:76-80
- [29] Moczydlowski E, Olivera BM, Gray WR, Strichartz GR. Discrimination of muscle and neuronal Na-channel subtypes by binding competition between [3H]saxitoxin and mu-conotoxins. *Proceedings of the National Academy of Sciences of the United States of America*. 1986;**83**:5321-5325
- [30] Cruz LJ, Gray WR, Olivera BM, Zeikus RD, Kerr L, Yoshikami D, Moczydlowski E. Conus geographus toxins that discriminate between neuronal and muscle sodium channels. *The Journal of Biological Chemistry*. 1985;**260**:9280-9288

- [31] Dib-Hajj SD, Yang Y, Black JA, Waxman SG. The Na(V)1.7 sodium channel: from molecule to man. *Nature Reviews Neuroscience*. 2013;**14**:49-62. DOI: 10.1038/nrn3404
- [32] Payandeh J, Scheuer T, Zheng N, Catterall WA. The crystal structure of a voltage-gated sodium channel. *Nature*. 2011;**475**:353-358. DOI: 10.1038/nature10238
- [33] Overington JP, Al-Lazikani B, Hopkins AL. How many drug targets are there? *Nature Reviews Drug Discovery*. 2006;**5**:993-996. DOI: 10.1038/nrd2199
- [34] McCusker EC, Bagn eris C, Naylor CE, Cole AR, D'Avanzo N, Nichols CG, Wallace BA. Structure of a bacterial voltage-gated sodium channel pore reveals mechanisms of opening and closing. *Nature Communications*. 2012;**3**:1102. DOI: 10.1038/ncomms2077
- [35] Sula A, Booker J, Ng LCT, Naylor CE, DeCaen PG, Wallace BA. The complete structure of an activated open sodium channel. *Nature Communications*. 2017;**8**:14205. DOI: 10.1038/ncomms14205
- [36] De Lera Ruiz M, Kraus RL. Voltage-gated sodium channels: Structure, function, pharmacology, and clinical indications. *Journal of Medicinal Chemistry*. 2015;**58**:7093-7118. DOI: 10.1021/jm501981g
- [37] Zhang X, Ren W, DeCaen P, Yan C, Tao X, Tang L, Wang J, Hasegawa K, Kumasaka T, He J, Wang J, Clapham DE, Yan N. Crystal structure of an orthologue of the NaChBac voltage-gated sodium channel. *Nature*. 2012;**486**:130-134. DOI: 10.1038/nature11054
- [38] Pless SA, Elstone FD, Niciforovic AP, Galpin JD, Yang R, Kurata HT, Ahern CA. Asymmetric functional contributions of acidic and aromatic side chains in sodium channel voltage-sensor domains. *The Journal of General Physiology*. 2014;**143**:645-656. DOI: 10.1085/jgp.201311036
- [39] Heinemann SH, Terlau H, St uhmer W, Imoto K, Numa S. Calcium channel characteristics conferred on the sodium channel by single mutations. *Nature*. 1992;**356**:441-443. DOI: 10.1038/356441a0
- [40] Agnew WS, Moore AC, Levinson SR, Raftery MA. Identification of a large molecular weight peptide associated with a tetrodotoxin binding protein from the electroplax of *Electrophorus electricus*. *Biochemical and Biophysical Research Communications*. 1980;**92**:860-866. DOI: 10.1016/0006-291X(80)90782-2
- [41] Miller JA, Agnew WS, Levinson SR. Principal glycopeptide of the tetrodotoxin/saxitoxin binding protein from *Electrophorus electricus*: Isolation and partial chemical and physical characterization. *Biochemistry*. 1983;**22**:462-470
- [42] Fozzard HA, Lipkind GM. The tetrodotoxin binding site is within the outer vestibule of the sodium channel. *Marine Drugs*. 2010;**8**:219-234. DOI: 10.3390/md8020219
- [43] Ahern CA, Eastwood AL, Dougherty DA, Horn R. Electrostatic contributions of aromatic residues in the local anesthetic receptor of voltage-gated sodium channels. *Circulation Research*. 2008;**102**:86-94. DOI: 10.1161/CIRCRESAHA.107.160663

- [44] Wang S-Y, Tikhonov DB, Mitchell J, Zhorov BS, Wang GK. Irreversible block of cardiac mutant Na⁺ channels by batrachotoxin. *Channels (Austin)*. n.d.;1:179-188
- [45] Du Y, Garden DP, Wang L, Zhorov BS, Dong K. Identification of new batrachotoxin-sensing residues in segment III S6 of the sodium channel. *The Journal of Biological Chemistry*. 2011;286:13151-13160. DOI: 10.1074/jbc.M110.208496
- [46] Strichartz GR. The inhibition of sodium currents in myelinated nerve by quaternary derivatives of lidocaine. *The Journal of General Physiology*. 1973;62:37-57
- [47] Armstrong CM, Bezanilla F. Charge movement associated with the opening and closing of the activation gates of the Na channels. *The Journal of General Physiology*. 1974;63:533-552
- [48] Oelstrom K, Goldschen-Ohm MP, Holmgren M, Chanda B. Evolutionarily conserved intracellular gate of voltage-dependent sodium channels. *Nature Communications*. 2014;5:3420. DOI: 10.1038/ncomms4420
- [49] West JW, Patton DE, Scheuer T, Wang Y, Goldin AL, Catterall WA. A cluster of hydrophobic amino acid residues required for fast Na⁽⁺⁾-channel inactivation. *Proceedings of the National Academy of Sciences of the United States of America*. 1992;89:10910-10914
- [50] Oxford GS, Wu CH, Narahashi T. Removal of sodium channel inactivation in squid giant axons by n-bromoacetamide. *The Journal of General Physiology*. 1978;71:227-247
- [51] Eaholtz G, Scheuer T, Catterall WA. Restoration of inactivation and block of open sodium channels by an inactivation gate peptide. *Neuron*. 1994;12:1041-1048
- [52] Jones DK, Peters CH, Allard CR, Claydon TW, Ruben PC. Proton sensors in the pore domain of the cardiac voltage-gated sodium channel. *The Journal of Biological Chemistry*. 2013;288:4782-4791. DOI: 10.1074/jbc.M112.434266
- [53] Cheng X, Dib-Hajj SD, Tyrrell L, te Morsche RH, Drenth JPH, Waxman SG. Deletion mutation of sodium channel NaV1.7 in inherited erythromelalgia: enhanced slow inactivation modulates dorsal root ganglion neuron hyperexcitability. *Brain*. 2011;134:1972-1986. DOI: 10.1093/brain/awr143
- [54] Bendahhou S, Cummins TR, Kula RW, Fu Y-H, Ptáček LJ. Impairment of slow inactivation as a common mechanism for periodic paralysis in DIIS4-S5. *Neurology*. 2002;58:1266-1272
- [55] Silva JR, Goldstein SAN. Voltage-sensor movements describe slow inactivation of voltage-gated sodium channels I: Wild-type skeletal muscle Na(V)1.4. *Journal of General Physiology*. 2013;141:309-321. DOI: 10.1085/jgp.201210909
- [56] Goldin AL, Barchi RL, Caldwell JH, Hofmann F, Howe JR, Hunter JC, Kallen RG, Mandel G, Meisler MH, Netter YB, Noda M, Tamkun MM, Waxman SG, Wood JN, Catterall WA. Nomenclature of voltage-gated sodium channels. *Neuron*. 2000;28:365-368. DOI: 10.1016/S0896-6273(00)00116-1

- [57] Isom LL, Ragsdale DS, De Jongh KS, Westenbroek RE, Reber BF, Scheuer T, Catterall WA. Structure and function of the beta 2 subunit of brain sodium channels, a transmembrane glycoprotein with a CAM motif. *Cell*. 1995;**83**:433-442
- [58] Yu FH, Westenbroek RE, Silos-Santiago I, McCormick KA, Lawson D, Ge P, Ferriera H, Lilly J, DiStefano PS, Catterall WA, Scheuer T, Curtis R. Sodium channel beta4, a new disulfide-linked auxiliary subunit with similarity to beta2. *The Journal of Neuroscience*. 2003;**23**:7577-7585
- [59] Morgan K, Stevens EB, Shah B, Cox PJ, Dixon AK, Lee K, Pinnock RD, Hughes J, Richardson PJ, Mizuguchi K, Jackson AP. Beta 3: An additional auxiliary subunit of the voltage-sensitive sodium channel that modulates channel gating with distinct kinetics. *Proceedings of the National Academy of Sciences of the United States of America*. 2000;**97**(5):2308-2313. DOI: 10.1073/pnas.030362197
- [60] Isom LL, De Jongh KS, Patton DE, Reber BF, Offord J, Charbonneau H, Walsh K, Goldin AL, Catterall WA. Primary structure and functional expression of the beta 1 subunit of the rat brain sodium channel. *Science*. 1992;**256**:839-842
- [61] Feng G, Deák P, Chopra M, Hall LM. Cloning and functional analysis of TipE, a novel membrane protein that enhances *Drosophila para* sodium channel function. *Cell*. 1995;**82**:1001-1011
- [62] Lee SH, Smith TJ, Ingles PJ, Soderlund DM. Cloning and functional characterization of a putative sodium channel auxiliary subunit gene from the house fly (*Musca domestica*). *Insect Biochemistry and Molecular Biology*. 2000;**30**:479-487
- [63] Molinarolo S, Lee S, Leisle L, Lueck JD, Granata D, Carnevale V, Ahern CA. Cross-Kingdom auxiliary subunit modulation of a voltage-gated Sodium channel. *The Journal of biological chemistry*. 2018;**293**(14):4981-4992. DOI: 10.1074/JBC.RA117.000852
- [64] Kazen-Gillespie KA, Ragsdale DS, D'Andrea MR, Mattei LN, Rogers KE, Isom LL. Cloning, localization, and functional expression of sodium channel beta1A subunits. *The Journal of Biological Chemistry*. 2000;**275**:1079-1088. DOI: 10.1074/JBC.275.2.1079
- [65] Hull JM, Isom LL. Voltage-gated sodium channel β subunits: The power outside the pore in brain development and disease. *Neuropharmacology*. 2018;**132**:43-57. DOI: 10.1016/j.neuropharm.2017.09.018
- [66] Brackenbury WJ, Isom LL. Na⁺ channel β subunits: Overachievers of the ion channel family. *Frontiers in Pharmacology*. 2011;**2**:53. DOI: 10.3389/fphar.2011.00053
- [67] Baroni D, Moran O. On the multiple roles of the voltage gated sodium channel β 1 subunit in genetic diseases. *Frontiers in Pharmacology*. 2015;**6**:108. DOI: 10.3389/fphar.2015.00108
- [68] O'Malley HA, Isom LL. Sodium channel β subunits: Emerging targets in channelopathies. *Annual Review of Physiology*. 2015;**77**:481-504. DOI: 10.1146/annurev-physiol-021014-071846

- [69] Drenth JPH, Waxman SG. Mutations in sodium-channel gene SCN9A cause a spectrum of human genetic pain disorders. *The Journal of Clinical Investigation*. 2007;**117**:3603-3610. DOI: 10.1172/JCI33297.type
- [70] Dib-Hajj SD, Binshtok AM, Cummins TR, Jarvis MF, Samad T, Zimmermann K. Voltage-gated sodium channels in pain states: Role in pathophysiology and targets for treatment. *Brain Research Reviews*. 2009;**60**:65-83. DOI: 10.1016/j.brainresrev.2008.12.005
- [71] Huang W, Liu M, Yan SF, Yan N. Structure-based assessment of disease-related mutations in human voltage-gated sodium channels. *Protein & Cell*. 2017;**8**:401-438. DOI: 10.1007/s13238-017-0372-z
- [72] Emery EC, Luiz AP, Wood JN. Nav1.7 and other voltage-gated sodium channels as drug targets for pain relief. *Expert Opinion on Therapeutic Targets*. 2016;**20**:975-983. DOI: 10.1517/14728222.2016.1162295
- [73] Fritz J, Wang KC, Carrino JA. Magnetic resonance neurography-guided nerve blocks for the diagnosis and treatment of chronic pelvic pain syndrome. *Neuroimaging Clinics of North America*. 2014;**24**:211-234. DOI: 10.1016/J.NIC.2013.03.028
- [74] Zorina-Lichtenwalter K, Parisien M, Diatchenko L. Genetic studies of human neuropathic pain conditions: A review. *Pain*. 2018;**159**:583-594. DOI: 10.1097/j.pain.0000000000001099
- [75] Yang Y, Wang Y, Li S, Xu Z, Li H, Ma L, Fan J, Bu D, Liu B, Fan Z, Wu G, Jin J, Ding B, Zhu X, Shen Y. Mutations in SCN9A, encoding a sodium channel alpha subunit, in patients with primary erythralgia. *Journal of Medical Genetics*. 2004;**41**:171-174
- [76] Cox JJ, Reimann F, Nicholas AK, Thornton G, Roberts E, Springell K, Karbani G, Jafri H, Mannan J, Raashid Y, Al-Gazali L, Hamamy H, Valente EM, Gorman S, Williams R, McHale DP, Wood JN, Gribble FM, Woods CG. An SCN9A channelopathy causes congenital inability to experience pain. *Nature*. 2006;**444**:894-898. DOI: 10.1038/nature05413
- [77] Nassar MA, Stirling LC, Forlani G, Baker MD, Matthews EA, Dickenson AH, Wood JN. Nociceptor-specific gene deletion reveals a major role for Nav1.7 (PN1) in acute and inflammatory pain. *Proceedings of the National Academy of Sciences*. 2004;**101**:12706-12711. DOI:10.1073/pnas.0404915101
- [78] Dib-Hajj SD, Tyrrell L, Cummins TR, Black JA, Wood PM, Waxman SG. Two tetrodotoxin-resistant sodium channels in human dorsal root ganglion neurons. *FEBS Letters*. 1999;**462**:117-120
- [79] Faber CG, Lauria G, Merkies ISJ, Cheng X, Han C, Ahn H-S, Persson A-K, Hoeijmakers JGJ, Gerrits MM, Pierro T, Lombardi R, Kapetis D, Dib-Hajj SD, Waxman SG. Gain-of-function Nav1.8 mutations in painful neuropathy. *Proceedings of the National Academy of Sciences of the United States of America*. 2012;**109**:19444-19449. DOI: 10.1073/pnas.1216080109
- [80] Huang J, Yang Y, Zhao P, Gerrits MM, Hoeijmakers JGJ, Bekelaar K, Merkies ISJ, Faber CG, Dib-Hajj SD, Waxman SG. Small-fiber neuropathy Nav1.8 mutation shifts activation

- to hyperpolarized potentials and increases excitability of dorsal root ganglion neurons. *Journal of Neuroscience*. 2013;**33**:14087-14097. DOI: 10.1523/JNEUROSCI.2710-13.2013
- [81] Han C, Vasylyev D, Macala LJ, Gerrits MM, Hoeijmakers JGJ, Bekelaar KJ, Dib-Hajj SD, Faber CG, Merkies ISJ, Waxman SG. The G1662S NaV1.8 mutation in small fibre neuropathy: impaired inactivation underlying DRG neuron hyperexcitability. *Journal of Neurology, Neurosurgery, and Psychiatry*. 2014;**85**:499-505. DOI: 10.1136/jnnp-2013-306095
- [82] Dib-Hajj SD, Black JA, Waxman SG. NaV1.9: A sodium channel linked to human pain. *Nature Reviews Neuroscience*. 2015;**16**:511-519. DOI: 10.1038/nrn3977
- [83] Wallace RH, Wang DW, Singh R, Scheffer IE, George AL, Phillips HA, Saar K, Reis A, Johnson EW, Sutherland GR, Berkovic SF, Mulley JC. Febrile seizures and generalized epilepsy associated with a mutation in the Na⁺-channel β 1 subunit gene SCN1B. *Nature Genetics*. 1998;**19**:366-370. DOI: 10.1038/1252
- [84] Escayg A, MacDonald BT, Meisler MH, Baulac S, Huberfeld G, An-Gourfinkel I, Brice A, LeGuern E, Moulard B, Chaigne D, Buresi C, Malafosse A. Mutations of SCN1A, encoding a neuronal sodium channel, in two families with GEFS+2. *Nature Genetics*. 2000;**24**:343-345. DOI: 10.1038/74159
- [85] Estacion M, O'Brien JE, Conravey A, Hammer MF, Waxman SG, Dib-Hajj SD, Meisler MH. A novel de novo mutation of SCN8A (Nav1.6) with enhanced channel activation in a child with epileptic encephalopathy. *Neurobiology of Diseases*. 2014;**69**:117-123. DOI: 10.1016/j.nbd.2014.05.017
- [86] Mantegazza M, Curia G, Biagini G, Ragsdale DS, Avoli M. Voltage-gated sodium channels as therapeutic targets in epilepsy and other neurological disorders. *Lancet Neurology*. 2010;**9**:413-424. DOI: 10.1016/S1474-4422(10)70059-4
- [87] Park DS, Fishman GI. SCN5A: The greatest HITS collection. *The Journal of Clinical Investigation*. 2018;**128**:913-915. DOI: 10.1172/JCI99927
- [88] Wang Q, Shen J, Splawski I, Atkinson D, Li Z, Robinson JL, Moss AJ, Towbin JA, Keating MT. SCN5A mutations associated with an inherited cardiac arrhythmia, long QT syndrome. *Cell*. 1995;**80**:805-811
- [89] Zimmer T, Surber R. SCN5A channelopathies—An update on mutations and mechanisms. *Progress in Biophysics and Molecular Biology*. 2008;**98**:120-136. DOI: 10.1016/j.pbiomolbio.2008.10.005
- [90] Cannon SC. From mutation to myotonia in sodium channel disorders. *Neuromuscular Disorders*. 1997;**7**:241-249
- [91] Meisler MH, Sprunger LK, Plummer NW, Escayg A, Jones JM. Ion channel mutations in mouse models of inherited neurological disease. *Annals of Medicine*. 1997;**29**:569-574
- [92] Kohrman DC, Smith MR, Goldin AL, Harris J, Meisler MH. A missense mutation in the sodium channel Scn8a is responsible for cerebellar ataxia in the mouse mutant jolting. *The Journal of Neuroscience*. 1996;**16**:5993-5999

- [93] Meisler MH, Plummer NW, Burgess DL, Buchner DA, Sprunger LK. Allelic mutations of the sodium channel SCN8A reveal multiple cellular and physiological functions. *Genetics*. 2004;**122**:37-45
- [94] Focken T, Liu S, Chahal N, Dauphinais M, Grimwood ME, Chowdhury S, Hemeon I, Bichler P, Bogucki D, Waldbrook M, Bankar G, Sojo LE, Young C, Lin S, Stuart N, Kwan R, Pang J, Chang JH, Safina BS, Sutherlin DP, Johnson JP, Dehnhardt CM, Mansour TS, Oballa RM, Cohen CJ, Robinette CL. Discovery of aryl sulfonamides as isoform-selective inhibitors of NaV1.7 with efficacy in rodent pain models. *ACS Medicinal Chemistry Letters*. 2016;**7**:277-282. DOI: 10.1021/acsmchemlett.5b00447
- [95] Bagal SK, Kemp MI, Bungay PJ, Hay TL, Murata Y, Payne CE, Stevens EB, Brown A, Blakemore DC, Corbett MS, Miller DC, Omoto K, Warmus JS. Discovery and optimization of potent and highly subtype selective Nav1.8 inhibitors with reduced cardiovascular liabilities. *Medchemcomm*. 2016;**7**:1925-1931. DOI: 10.1039/C6MD00281A
- [96] Narahashi T. Tetrodotoxin: A brief history. *Proceedings of the Japan Academy. Series B, Physical and Biological Sciences*. 2008;**84**:147-154
- [97] French RJ, Worley JF, Krueger BK. Voltage-dependent block by saxitoxin of sodium channels incorporated into planar lipid bilayers. *Biophysical Journal*. 1984;**45**:301-310. DOI: 10.1016/S0006-3495(84)84156-9
- [98] Wilson MJ, Yoshikami D, Azam L, Gajewiak J, Olivera BM, Bulaj G, Zhang M-M. μ -Conotoxins that differentially block sodium channels NaV1.1 through 1.8 identify those responsible for action potentials in sciatic nerve. *Proceedings of the National Academy of Sciences of the United States of America*. 2011;**108**:10302-10307. DOI: 10.1073/pnas.1107027108
- [99] Leipold E, Hansel A, Olivera BM, Terlau H, Heinemann SH. Molecular interaction of delta-conotoxins with voltage-gated sodium channels. *FEBS Letters*. 2005;**579**:3881-3884. DOI: 10.1016/j.febslet.2005.05.077
- [100] Gajewiak J, Azam L, Imperial J, Walewska A, Green BR, Bandyopadhyay PK, Raghuraman S, Ueberheide B, Bern M, Zhou HM, Minassian NA, Hagan RH, Flinspach M, Liu Y, Bulaj G, Wickenden AD, Olivera BM, Yoshikami D, Zhang M-M. A disulfide tether stabilizes the block of sodium channels by the conotoxin μ OS-GVIIJ. *Proceedings of the National Academy of Sciences of the United States of America*. 2014;**111**:2758-2763. DOI: 10.1073/pnas.1324189111
- [101] Strachan LC, Lewis RJ, Nicholson GM. Differential actions of pacific ciguatoxin-1 on sodium channel subtypes in mammalian sensory neurons. *The Journal of Pharmacology and Experimental Therapeutics*. 1999;**288**:379-388
- [102] Wang S-Y, Mitchell J, Tikhonov DB, Zhorov BS, Wang GK. How batrachotoxin modifies the sodium channel permeation pathway: Computer modeling and site-directed mutagenesis. *Molecular Pharmacology*. 2005;**69**:788-795. DOI: 10.1124/mol.105.018200

- [103] Wang GK, Wang S-Y. Veratridine block of rat skeletal muscle Nav1.4 sodium channels in the inner vestibule. *Journal of Physiology*. 2003;**548**:667-675. DOI: 10.1113/jphysiol.2002.035469
- [104] Ghiasuddin SM, Soderlund DM. Mouse brain synaptosomal sodium channels: Activation by aconitine, batrachotoxin, and veratridine, and inhibition by tetrodotoxin. *Comparative Biochemistry and Physiology*. C. 1984;**77**:267-271
- [105] Cao Z, Gerwick WH, Murray TF. Antillatoxin is a sodium channel activator that displays unique efficacy in heterologously expressed rNav1.2, rNav1.4 and rNav1.5 alpha subunits. *BMC Neuroscience*. 2010;**11**:154. DOI: 10.1186/1471-2202-11-154
- [106] Jansen SA, Kleerekooper I, Hofman ZLM, Kappen IFPM, Stary-Weinzinger A, van der Heyden MAG. Grayanotoxin poisoning: 'Mad Honey Disease' and beyond. *Cardiovascular Toxicology*. 2012;**12**:208-215. DOI: 10.1007/s12012-012-9162-2
- [107] Bosmans F, Tytgat J. Voltage-gated sodium channel modulation by scorpion alpha-toxins. *Toxicon*. 2007;**49**:142-158. DOI: 10.1016/j.toxicon.2006.09.023
- [108] Moran Y, Gordon D, Gurevitz M. Sea anemone toxins affecting voltage-gated sodium channels—Molecular and evolutionary features. *Toxicon*. 2009;**54**:1089-1101. DOI: 10.1016/j.toxicon.2009.02.028
- [109] Pedraza Escalona M, Possani LD. Scorpion beta-toxins and voltage-gated sodium channels: interactions and effects. *Frontiers in Bioscience (Landmark Ed.)*. 2013;**18**:572-587
- [110] Middleton RE, Warren VA, Kraus RL, Hwang JC, Liu CJ, Dai G, Brochu RM, Kohler MG, Gao Y-D, Garsky VM, Bogusky MJ, Mehl JT, Cohen CJ, Smith MM. Two tarantula peptides inhibit activation of multiple sodium channels. *Biochemistry*. 2002;**41**:14734-14747
- [111] Xiao Y, Luo X, Kuang F, Deng M, Wang M, Zeng X, Liang S. Synthesis and characterization of huwentoxin-IV, a neurotoxin inhibiting central neuronal sodium channels. *Toxicon*. 2008;**51**:230-239. DOI: 10.1016/j.toxicon.2007.09.008
- [112] Bosmans F, Swartz KJ. Targeting voltage sensors in sodium channels with spider toxins. *Trends in Pharmacological Sciences*. 2010;**31**:175-182. DOI: 10.1016/j.tips.2009.12.007
- [113] Green BR, Olivera BM. Venom Peptides From Cone Snails. *Current Topics in Membrane*. 2016;**78**:65-86. DOI: 10.1016/bs.ctm.2016.07.001
- [114] Dechraoui MY, Naar J, Pauillac S, Legrand AM. Ciguatoxins and brevetoxins, neurotoxic polyether compounds active on sodium channels. *Toxicon*. 1999;**37**:125-143
- [115] Hasson A, Fainzilber M, Gordon D, Zlotkin E, Spira ME. Alteration of sodium currents by new peptide toxins from the venom of a molluscivorous *Conus* snail. *The European Journal of Neuroscience*. 1993;**5**:56-64
- [116] Tanelian DL, Brose WG. Neuropathic pain can be relieved by drugs that are use-dependent sodium channel blockers: Lidocaine, carbamazepine, and mexiletine. *Anesthesiology*. 1991;**74**:949-951

- [117] Song JH, Ham SS, Shin YK, Lee CS. Amitriptyline modulation of Na⁺ channels in rat dorsal root ganglion neurons. *European Journal of Pharmacology*. 2000;**401**:297-305
- [118] Yasam VR, Jakki SL, Senthil V, Eswaramoorthy M, Shanmuganathan S, Arjunan K, Nanjan M. A pharmacological overview of lamotrigine for the treatment of epilepsy. *Expert Review of Clinical Pharmacology*. 2016;**9**:1533-1546. DOI: 10.1080/17512433.2016.1254041
- [119] Ragsdale DS, McPhee JC, Scheuer T, Catterall WA. Molecular determinants of state-dependent block of Na⁺ channels by local anesthetics. *Science*. 1994;**265**:1724-1728
- [120] Grace AA, Camm AJ. Quinidine. *The New England Journal of Medicine*. 1998;**338**:35-45. DOI: 10.1056/NEJM199801013380107
- [121] Watanabe H, Chopra N, Laver D, Hwang HS, Davies SS, Roach DE, Duff HJ, Roden DM, Wilde AAM, Knollmann BC. Flecainide prevents catecholaminergic polymorphic ventricular tachycardia in mice and humans. *Nature Medicine*. 2009;**15**:380-383. DOI: 10.1038/nm.1942
- [122] Pfizer. Efficacy of PF-05089771 in treating postoperative dental pain. *ClinicalTrials.Gov*. 2012. <https://clinicaltrials.gov/ct2/show/NCT01529346> [Accessed: March 18, 2018]
- [123] Ahuja S, Mukund S, Deng L, Khakh K, Chang E, Ho H, Shriver S, Young C, Lin S, Johnson JP Jr, Wu P, Li J, Coons M, Tam C, Brillantes B, Sampang H, Mortara K, Bowman KK, Clark KR, Estevez A, Xie Z, Verschoof H, Grimwood M, Dehnhardt C, Andrez JC, Focken T, Sutherlin DP, Safina BS, Starovasnik MA, Ortwine DF, Franke Y, Cohen CJ, Hackos DH, Koth CM, Payandeh J. Structural basis of Nav1.7 inhibition by an isoform-selective small-molecule antagonist. *Science* (80-.). 2015;**350**:aac5464. DOI: 10.1126/science.aac5464
- [124] Jarvis MF, Honore P, Shieh CC, Chapman M, Joshi S, Zhang XF, Kort M, Carroll W, Marron B, Atkinson R, Thomas J, Liu D, Krambis M, Liu Y, McGaraughty S, Chu K, Roeloffs R, Zhong C, Mikusa JP, Hernandez G, Gauvin D, Wade C, Zhu C, Pai M, Scanio M, Shi L, Drizin I, Gregg R, Matulenko M, Hakeem A, Gross M, Johnson M, Marsh K, Wagoner PK, Sullivan JP, Faltynek CR, Krafte DS. A-803467, a potent and selective Nav1.8 sodium channel blocker, attenuates neuropathic and inflammatory pain in the rat. *Proceedings of the National Academy of Sciences of the United States of America*. 2007;**104**:8520-8525. DOI: 10.1073/pnas.0611364104